"IDENTIFYING MOLECLES REQUIRED FOR BLOOD-BRAIN BARRIER DYSFUNCTION DURING DISEASE"

FINAL REPORT

by

Kaja BAJC

Master programme
Medical and Pharmaceutical Biotechnology
IMC Fachhochschule Krems
(University of Applied Sciences)

for

Austrian Marshall Plan Foundation

Internal supervisor: Barbara Entler, Prof.(FH) Dr.

External supervisor: Richard Daneman, PhD, Assistant Professor

Submitted on: 28.03.2017

Acknowledgements

First of all I would like to thank my supervisor Dr. Richard Daneman for not missing an email and giving me the opportunity to join his research group. There are no words to express my gratitude for all of his guidance and trust during my time there. He has not only helped me grow into being a better researcher but also became someone who influenced that part of my life immensely.

Additionally, I would also like to thank my internal supervisor Prof. Barbara Entler for all her help during my time away and with the master thesis.

Special thanks goes to my dear friend Catie Profaci, the egg of my plant, for successfully sneaking into every memory I have from San Diego and making those eight months unforgettable. For all her time and patience while teaching me the necessary techniques and all the help on the project and writing the master thesis.

In addition, I want to thank my colleagues and friends in Daneman lab for creating such an inspiring environment and making me feel home away from home.

I owe a great debt of thanks to my family and friends back at home. Their love and support during my adventures means the world to me.

Finally, this project would have not been possible without the financial support of the Austrian Marshall Plan Foundation. I feel extremely lucky and honored to be called a Marshall Plan Foundation fellow.

Abstract

Blood-brain barrier (BBB) is a term describing the unique properties of endothelial cells forming the walls of blood vessels of CNS vasculature. Blood-brain barrier has two main roles - to strictly regulate the flow of ions, molecules and cells between blood and the brain and to maintain brain homeostasis that is essential for proper neuronal function. However, BBB breakdown is a component of many neurological diseases such as multiple sclerosis, stroke, epilepsy, traumatic brain injury and contribute greatly to the disease pathology. The molecular mechanisms driving the BBB breakdown and repair are still not completely understood. Here we demonstrate that *Pdlim1* is one of the genes upregulated in mouse models of all four diseases; it is highly expressed in the blood vessels in the areas of BBB breakdown indicating to a potential correlation between PDLIM1 and BBB breakdown. However, there is a lack of data regarding the function of PDLIM1. With the use of two *in vivo* models we reveal that although upregulation does not lead to BBB breakdown, it might be involved in inflammation and/or myelination in EAE – mouse model of multiple sclerosis. To further investigate the role of PDLIM1 at the BBB we show that PDLIM1 is also expressed in cell culture and optimize parameters for successful PDLIM1 siRNA knockdown in primary brain endothelial cell culture; the first step needed for investigating the function of PDLIM1 *in vitro*.

Table of Contents

List of Figures and Illustrations

List of tables

List of Abbreviations

ALP	Actinin-associated LIM Protein
ALS	Amyotrophic Lateral Sclerosis
BBB	Blood-Brain Barrier
BECs	Brain Endothelial Cells
bFGF	basic Fibroblast Growth Factor
BM	Basement Membrane
CFA	Complete Freund’s Adjuvant
CNS	Central Nervous System
DMEM	Dulbecco's Modified Eagle Medium
DPBS	Dulbecco's Phosphate-Buffered Saline
EAE	Experimental Autoimmune Encephalomyelitis
EC	Endothelial Cells
FACS	Fluorescence-Activated Cell Sorting
GAPDH	Glyceraldehyde 3-Phosphate Dehydrogenase
GFP	Green Fluorescent Protein
GLUT-1	Glucose Transporter 1
HET	Heterozygote
ICAM1	Intercellular Adhesion Molecule-1
IL-1	Interleukin-1
IL-6	Interleukin-6
kDa	kiloDalton
KO	Knockout
MCAO	Middle Cerebral Artery Occlusion
MMPs	Matrix-Metalloproteinases
MOG	Myelin Oligodendrocyte Glycoprotein
MRI	Magnetic Resonance Imaging
MS	Multiple Sclerosis
NF-kB	Nuclear Factor Kappa Beta
NVU	Neurovascular unit
OCT	Optimal Cutting Temperature compound

OPC	Oligodendrocyte Precursor Cell
$p75^{NTR}$	p75 Neurotrophin Receptor
PBS	Phosphate-Buffered Saline
PDLIM1	PDZ and LIM domain protein 1
Pen/Strep	Penicillin/Streptomycin
PFA	Paraformaldehyde
PGP	P-Glycoprotein
PTX	Pertussis Toxin
RNA-Seq	RNA Sequencing
ROS	Reactive Oxygen Species
RT	Room Temperature
SDS-PAGE	Sodium Dodecyl Sulfate Polyacrylamide Gel Electrophoresis
siRNA	small Interfering RNA
TBI	Traumatic Brain Injury
TBST	Tris Buffered Saline with Tween
TJ	Tight Junction
TNF-alpha	Tumor Necrosis Factor alpha
TRE	Tetracycline Response Element
tTA	tetracycline-controlled Transactivator protein
VCAM1	Vascular Cell Adhesion Molecule 1
VEGF	Vascular Endothelial Growth Factor
WT	Wild Type

1 Introduction

Most of the body functions are controlled and carried out by the central nervous system (CNS), which is made up of the brain and spinal cord. Its damage leads to many neurological diseases. Therefore, there must be a strict regulation of substances that interact with it, because any foreign molecules can be harmful for the CNS. In addition, maintaining ionic homeostasis of extracellular fluid is important for proper neuronal function. In order to restrict access to the CNS and maintain homeostasis, the body has set up a complex interface between blood and the parenchyma, called the blood-brain barrier (BBB). Therefore, the BBB is crucial for maintaining of CNS homeostasis and preventing the entry of pathogens, toxins and own immune cells that could have a damaging and irreversible effect on neurons (Gloor et al. 2001). Dysfunction of the BBB has been associated with many CNS diseases. This master thesis will focus on BBB dysfunction in multiple sclerosis (MS), stroke, traumatic brain injury (TBI) and epilepsy. The experimental part will investigate the role of the gene *Pdlim1*, whose upregulation in endothelial cells was observed in mouse models of all of these diseases (Figure 1).

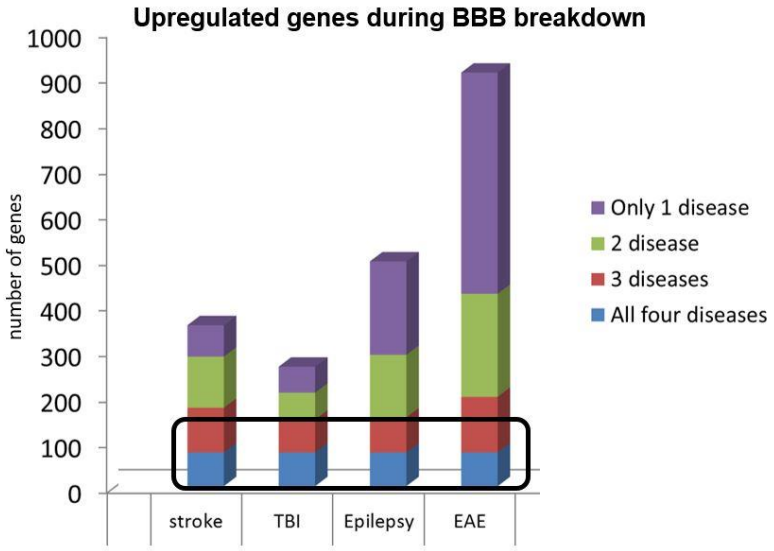

Figure 1: Upregulated genes during BBB breakdown.
The graph is representing results from RNA-Seq data of FACS-purified endothelial cells during BBB breakdown in each of the disease. The x-axis is showing separate bars for each of the disease. Number of genes upregulated in all 4 diseases is seen in blue color and *Pdlim1* is one of those genes. Data is courtesy of Richard Daneman's lab at University of California, San Diego.

1.1 Blood-brain barrier

The first indication that there might be a barrier preventing substances to enter the brain was observed more than a century ago by German scientist Paul Ehrlich. His intravenous injections of dyes resulted in staining of all the tissues in the body, except the brain (Ehrlich 1885). After that, many scientists reported similar observations, but the explanation for it remained controversial (Saunders et al. 2014). The term BBB was long poorly understood and thought of only as being a "wall" between blood and the CNS. With emerging discoveries about BBB structure and function a more complex explanation was needed. What is defined as BBB is a set of properties that are distinct for endothelial cells forming the walls of blood vessels in CNS vasculature, in order to restrict the movement of ions, molecules and cells between blood and the CNS.

1.1.1 Neurovascular unit

One of the properties that make the endothelial cells (EC) of the BBB unique is that the adjacent cells are held together by tight junctions. The presence of tight junction strictly limits the paracellular diffusion of compounds between them (Luissint et al. 2012; Brightman & Reese 1969). Transcytosis across these cells is also minimized, therefore limiting the transcellular movement of molecules into the CNS (Rubin & Staddon 1999). While blood gasses such as oxygen and carbon dioxide can diffuse through by moving down the concentration gradient, the supply of other essential nutrients to the CNS such as glucose and amino acids relies on the expression of specific transporters on EC (Abbott et al. 2010). Passive diffusion of any unwanted solutes/molecules/substances that could harm the CNS is prevented by efflux transporters (Löscher & Potschka 2005). Endothelial cells also express low rates of leukocyte adhesion molecules (LAMs), subsequently decreasing the immune surveillance and possibility of immune cells to enter the BBB. Some of the properties of EC are presented on Figure 2. The detailed description of these properties is beyond the scope of this master thesis and is summarized well in recent reviews (Daneman & Prat 2015; Zhao et al. 2015; Abbott et al. 2010).

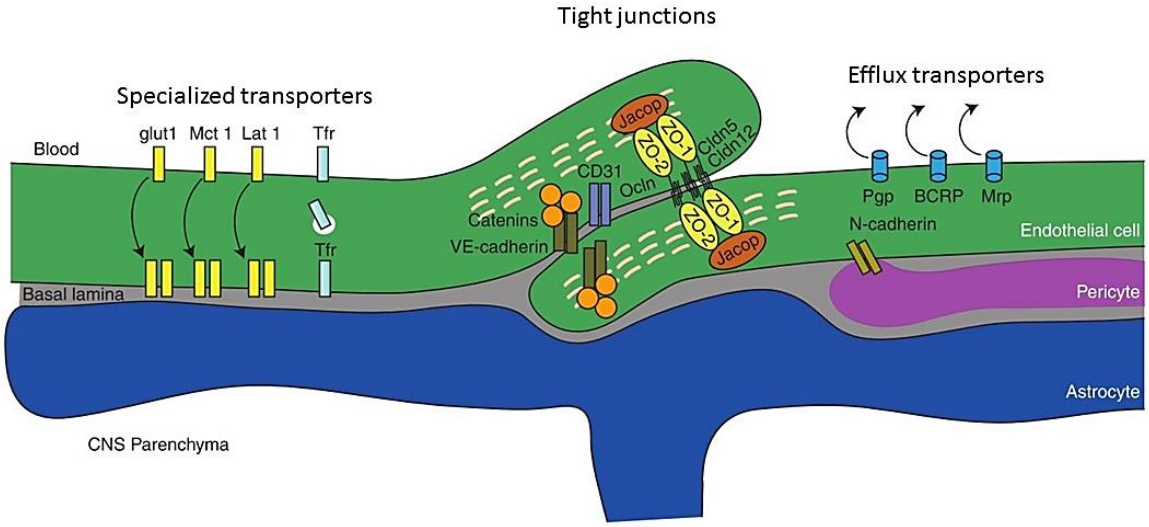

Figure 2: Schematic representation of BBB molecules.
Specialized transporters: Glut-1 (glucose transporter 1), Mct1 (Monocarboxylate transporter 1), Lat1 (L-type amino acid transporter 1), Tfr (transferrin receptor). Tight junction molecules: VE (vascular endothelial) – cadherin, Ocln (occludin), Cldn (claudin), ZO (zona occuldens proteins). Efflux transporters: Pgp (P-glycoprotein), BCRP (breast cancer resistance protein), Mrp (Multidrug resistance protein), N (neural) – cadherin. (Daneman & Prat 2015)

Although most of the properties of BBB are attributed to CNS endothelial cells, the regulation of them is maintained through interaction with other cell types present (Figure 3). Endothelial cells are forming the wall that is surrounding the lumen of vascular tubes. Pericytes are covering most of the ablumenal surface of endothelial cells and are embedded together with endothelial cells by basement membrane (BM). BM is made up of laminins, collagen and other extracellular matrix secreted by EC, pericytes and astrocytes. Astrocytes use their end foot processes for connection to basement membrane and neurons. Together with microglia, that are representing the immune surveillance in the brain, this complex network of interactions between the above mentions cell types is commonly referred to as neurovascular unit (Zhao et al. 2015; Hawkins & Davis 2005).

Beside EC, other cell types in the neurovascular unit contribute to the maintenance of a functional BBB. Pericytes have been shown to have a considerable role in BBB formation and angiogenesis in the development of CNS vasculature (Daneman et al. 2010) They have also been associated with regulation of capillary diameter and blood flow, as well as expressing phagocytotic properties. (Winkler et al. 2011).

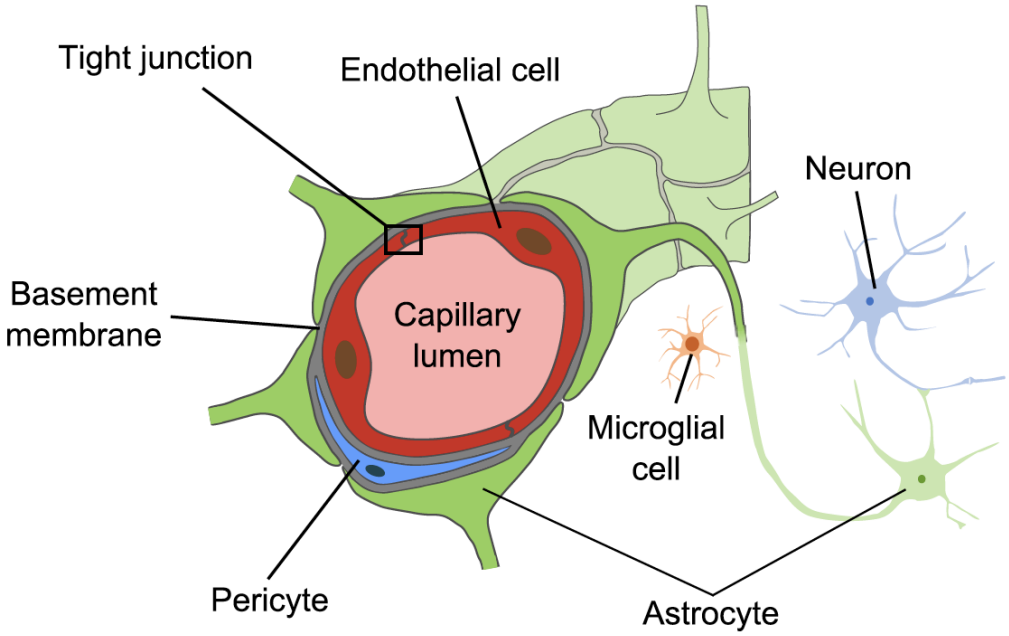

Figure 3: Schematic representation of major cell types in neurovascular unit (NVU) Endothelial cells (red), basement membrane (grey), pericytes (blue), astrocytes (green), neuron (blue), microglia (orange). (Heye et al. 2014)

Basement membrane covering CSN blood vessels consist of two layers: the inner endothelial BM (secreted by EC and pericytes) and outer parenchymal BM (secreted by astrocytes). These two BMs present an additional obstacle for crossing the barrier to CNS and act as a binding surface for interacting molecules and cells (del Zoppo et al. 2006; Sorokin 2010).

Connection of neuronal network with vasculature is mediated by astrocytes. Astrocytes use their cellular processes to surround neuronal synapses on one side and for coupling them to the BM on the other side. This positioning allow them to respond to neuronal stimuli and release metabolites for regulation of blood vessel diameter in response to changes in blood flow (Attwell et al. 2010). Furthermore, the expression of water channel aquaporin 4 on their end feet processes indicates their involvement in regulating CNS water homeostasis (Haj-Yasein et al. 2011)

Microglia are immune cells of CNS. Besides their role as immune surveillance and phagocytotic agents, they have been implicated in BBB integrity, especially needed for rapid resealing of the barrier after BBB breakdown (Lou et al. 2016).

1.2 BBB dysfunction/breakdown

It is important to understand that the meaning of BBB breakdown can mean any change in BBB properties (disruption of TJ, higher rates of transcytosis, change in transport properties, leukocyte infiltration) that can lead to disruption of CNS homeostasis and/or infiltration of cells to the CNS. By that, it is said that BBB becomes leaky, a feature that is not observed in fully functional BBB in health (Daneman 2012). BBB breakdown has been associated with many CNS disorders. It has been demonstrated that the breakdown plays a significant role in multiple sclerosis (Minagar & Alexander 2003; Alvarez et al. 2011), stroke (Sandoval & Witt 2008), traumatic brain injury (Alluri et al. 2015) and epilepsy (Oby & Janigro 2006). These diseases will be discussed later. The implication that BBB dysfunction is involved in neurodegenerative diseases such as Alzheimer's diseases, Parkinson's disease and Amyotrophic lateral sclerosis (ALS) is still debatable, where the exact role and whether the breakdown act as a cause or consequence in this diseases, is still unknown. (Erickson & Banks 2013; Zlokovic 2008; Garbuzova-Davis et al. 2012; Evans et al. 2013).

Although this breakdown and entrance of immune cells to the CNS may be necessary to repair the injury and debris clearance the prolonged leakage of plasma proteins and water into extracellular space can have more damaging consequences e.g. increased brain volume (vasogenic edema). Progressive swelling because of vasogenic edema can result in increased intracranial pressure and subsequently herniation of CNS tissue. Furthermore, cerebral perfusion can decrease, leading to tissue ischemia. In addition, in case of long standing cases of edema, myelin sheaths can become fragmented and neurons damaged. Vasogenic edema can ultimately result in death (Nag et al. 2009; Unterberg et al. 2004).

Most common method for measuring BBB disruption in humans involves injecting patients with gadolinium, followed by gadolinium-enhanced magnetic resonance imaging (MRI). Gadolinium is a small hydrophilic molecule, incapable of crossing functional BBB. If there is a BBB disruption, gadolinium will leak into the brain, and those areas will appear brighter on contrast enhanced image.

For measuring disruption of BBB in animal models, animals are injected with fluorescent or radioactive labeled tracer. Examples include Evan's blue dye, sodium fluorescein and labeled dextrans. Figure 4 is showing various mouse organs after an injection of Evan's blue dye in a mouse with intact BBB.

Figure 4: Mouse organs after Evan's blue injection.
If the BBB is intact, the dye penetrates in all tissues except the brain. In the image organs such as skin, intestine, kidney and liver are shown colored in blue, while brain is not colored. Image is courtesy of Richard Daneman.

For the practical work in this thesis, BBB leakage in mice is detected by giving trans-cardiac perfusion using tracer molecule Sulfo-NHS-biotin. Streptavidin, which is a protein biotin binds, is used for immunostaining of postmortem tissue and leakage is detected by measuring fluorescence (Figure 5).

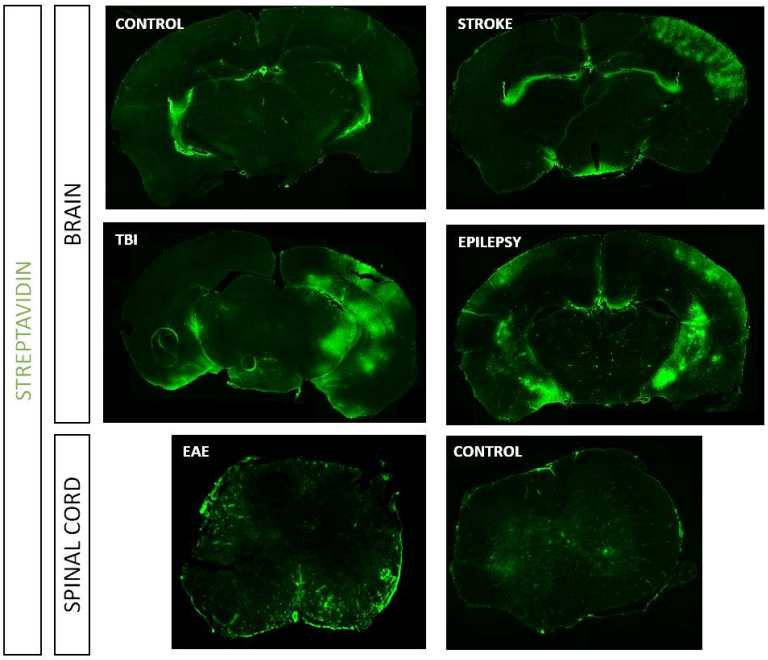

Figure 5: BBB breakdown in disease.
Brains and spinal cord from disease models of stroke, traumatic brain injury, epilepsy and EAE are stained against biotin. Green areas are representing BBB leakage. Biotin is a tracer molecule that mice were given by trans-cardiac perfusion. BBB permeability to biotin is increased at the areas of breakdown, indicating leakage. Upper panel is showing images of BBB breakdown in the brain of mouse models of stroke, TBI and epilepsy. Control brain are from C57BL/6 mouse. Lower panel is showing spinal cord of EAE and control mouse.

1.2.1 Multiple sclerosis

Multiple sclerosis is an autoimmune disease in which immune cells infiltrate CNS and attack myelin sheaths enveloping axons, resulting in formation of demyelinating lesions in the white matter. Patients with MS have impaired motor and sensory functions. Multiple sclerosis is thought to be driven by autoreactive T-cells, but the role of B cells is also emphasized, as there is increased synthesis and presence of antibodies in MS patients (Frohman et al. 2006).

BBB breakdown is one of the earliest events seen in MS and is necessary for infiltration of immune cells and progression of disease. Analysis of postmortem lesions demonstrated the presence of abnormal tight junctions and increase in serum components (Kirk et al. 2003; Padden et al. 2007). Interestingly, while BBB leakage plays a major role in development of new lesions, the leakage decreases later in disease progression and is rarely detected in older lesions (Harris et al. 1991). A theory based on gadolinium-enhanced MRI is proposing that BBB leakage gets repaired, while trapping immune cells in the CNS and contributing to progressing MS (Bradl & Lassmann 2009). There is no doubt that BBB breakdown is the hallmark of MS, however, it is still debatable whether the breakdown is the initial event preceding the formation of lesions (Guttmann et al. 2016).

Many of the studies of MS are done on mouse models such as experimental autoimmune encephalomyelitis (EAE), as its observed pathologies in mice are strongly similar to those in CNS of MS patients. EAE is induced by active or passive immunization. In the practical work of this thesis, EAE is induced by active immunization with direct injection of myelin antigen in an adjuvant (McCarthy et al. 2012).

1.2.2 Stroke

Ischemic stroke is a neurologic deficit in which regions of the brain are deprived of blood flow due to a blockage in the blood vessel supplying blood to the brain. Ischemic stroke has two different pathological phases – ischemia, leading to the loss of oxygen and nutrients to brain tissue, and reperfusion, restoring of the blood supply for tissue survival, which can cause even more tissue damage (Sandoval & Witt

2008). In animals, ischemic stroke is commonly modeled using middle cerebral artery occlusion (MCAO) followed by reperfusion. Work on different animal models of stroke demonstrated that BBB breakdown during ischemia/reperfusion occurs in phases, commonly referred to as biphasic opening of the barrier. The first BBB breakdown occurs within hours after primary insult, resulting in leakage. This leakage then subsides and reappears the next day due to the second BBB opening. (Huang et al. 1999; Kuroiwa et al. 1985). However, while underlying mechanisms of BBB breakdown in stroke are still not well understood, an increase in transcytosis was demonstrated as being the first event in early phase of reperfusion, followed by changes in expression of tight junction proteins in the late phase (Knowland et al. 2014).

1.2.3 TBI

Traumatic brain injury is a complex pathological condition caused by an external force to the brain. Immediately following impact, primary injuries such as tissue and blood vessel damage occur, leading to onset of secondary injuries, including BBB breakdown, that take place hours to days after primary insult (Alluri et al. 2015). BBB breakdown in TBI shares some common features with the breakdown in stroke. The breakdown is not involved in etiology of disease and follows a biphasic opening pattern where the first breakdown is seen hours and the second one a few days after the insult (Huang et al. 1999). What causes BBB dysfunction is also not well defined, although there is some evidence that Substance P which is released in TBI increases BBB permeability (Donkin et al. 2009).

1.2.4 Epilepsy

Epilepsy is a neurological disorder that causes seizures. Although the connection between epilepsy and BBB dysfunction is indisputable, it is still not clear how the breakdown of the barrier contributes to the disease pathology (Oby & Janigro 2006b). There has been some evidence that BBB dysfunction contributes to the onset of seizures, supported by a study showing that osmotic disruption of BBB leads to seizures in patients (Marchi et al. 2007). In addition, the importance of Glut-1 has also been highlighted. Glut-1 is one of the transporters on the surface of ECs,

responsible for the glucose supply to the brain. A defect in Glut-1 is a feature of Glut-1 deficiency syndrome, resulting in impaired energetic supply to the brain and consequently seizures (De Vivo et al. 1991). Furthermore, seizures are commonly observed in disease conditions such *as* stroke, TBI, and CNS infections, all of them associated with BBB breakdown.

1.3 PDLIM1

PDLIM1 is composed of 329 amino acids with a molecular mass of 36 kDa (Uniprot ID: O00151). It was first isolated and characterized as CLP-36 from rat hepatocytes, where it was down-regulated during chemical hypoxia (Wang et al. 1995). PDLIM1 (synonyms CLP36, Elfin, CLIM1) is one of the 10 proteins characterized as a PDZ and LIM domain protein. More specifically it is a member of ALP (actinin-associated LIM protein) protein subfamily. PDZ/LIM domain proteins consist of one amino terminal PDZ domain and one or more carboxy-terminal LIM domains and have been shown to influence the actin cytoskeleton by acting as a cytoskeletal adaptor proteins (te Velthuis & Bagowski 2007). Early in vitro studies established the interaction of PDLIM1 with the cytoskeleton and demonstrated its association with actin filaments and stress fibers through interaction with α actinin-1 and α actinin-4 (both non-muscle actinins), and α actinin-2 (skeletal and cardiac muscle actinin) (Bauer et al. 2000; Vallenius et al. 2000; Kotaka et al. 2000). Although the interaction with actinins was confirmed in many studies, the exact role of PDLIM1 is still unknown.

Previous studies in mice and rats showed that PDZ and LIM domain proteins are expressed predominately in skeletal muscle, but in contrast PDLIM1 expression is also observed in non-muscle tissue such as liver, lungs and other epithelial cells (Vallenius et al. 2000; Vallenius et al. 2004; Wang et al. 1995). There is a lack of data regarding the expression and function of PDLIM1 in nervous system, possibly because PDLIM1 is expressed there to a lesser extent (Figure 6). Report from one group detected very low levels of PDLIM1 in CNS of adult rats but showed its expression in peripheral nerve system predominantly in rat sensory ganglia and increase of expression in dorsal root ganglia after sciatic nerve injury. (Ohno et al.

2009). Same group later detected that in dorsal root ganglia, PDLIM1 forms a complex with another actin binding protein – palladin and suggested its role in neurite outgrowth, possibly by influencing the cytoskeletal rearrangement in nerve regeneration (Hasegawa et al. 2010).

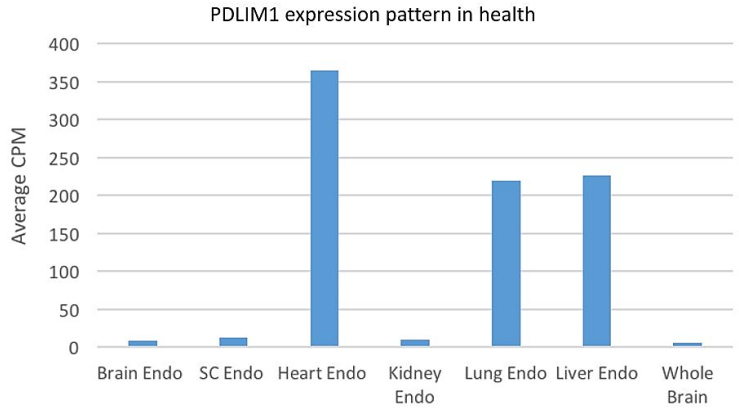

Figure 6: PDLIM1 expression pattern in health.
The graph is representing results of endothelial cell purification followed by RNA-Seq for PDLIM1 expression in different mouse tissue. The highest expression is observed in heart, followed by lung and liver endothelial cells. Very low CPM is detected in kidney, spinal cord and brain endothelial cells. Results for whole brain CMP are also presented, demonstrating that most of the PDLIM1 expression in brain corresponds to expression in brain endothelial cells. CPM = Counts Per Million Data is courtesy of Richard Daneman's laboratory at University of California, San Diego.

Later studies implicated the role of PDLIM1 in cancer progression. PDLIM1 expression was found to be highly upregulated in breast cancer, and further research highlighted PDLIM1/α-actinin complex as a factor in cell migration, invasion and metastasis (Liu et al. 2015). Furthermore, in one study PDLIM1 was shown to be critical for glioma invasion *in vivo* and *in vitro*, by acting as a signaling adaptor protein for p75 neurotrophin receptor (Ahn et al. 2016). Two recent articles are of great importance, both suggesting novel roles of PDLIM1. One demonstrated that in colon cancer PDLIM1 inhibits beta-catenin mediated transcription (Chen et al. 2016). Wnt/beta-catenin signaling is required for BBB formation and maintenance (Daneman et al. 2009), suggesting that perhaps upregulation of PDLIM1 in CNS endothelial cells leads to BBB dysfunction by inhibiting Wnt signaling. Second one demonstrated that PDLIM1 negatively regulates NF-κ B-mediated inflammatory signaling in the cytoplasm, suggesting that it might have a role in suppressing NF-κ B-mediated signaling and inflammation. PDLIM1 was shown to interact with p65 subunit and prevent its nuclear translocation from the cytoplasm (Ono et al. 2015).

As mentioned in the introduction (Figure 1), our findings demonstrated that *Pdlim1* is one of the genes upregulated during BBB breakdown in disease models of stroke, TBI, epilepsy and EAE. PDLIM1 expression at different timepoint of each disease model is presented in Figure 7. This data is suggesting the possible role of PDLIM1 in BBB dysfunction in disease.

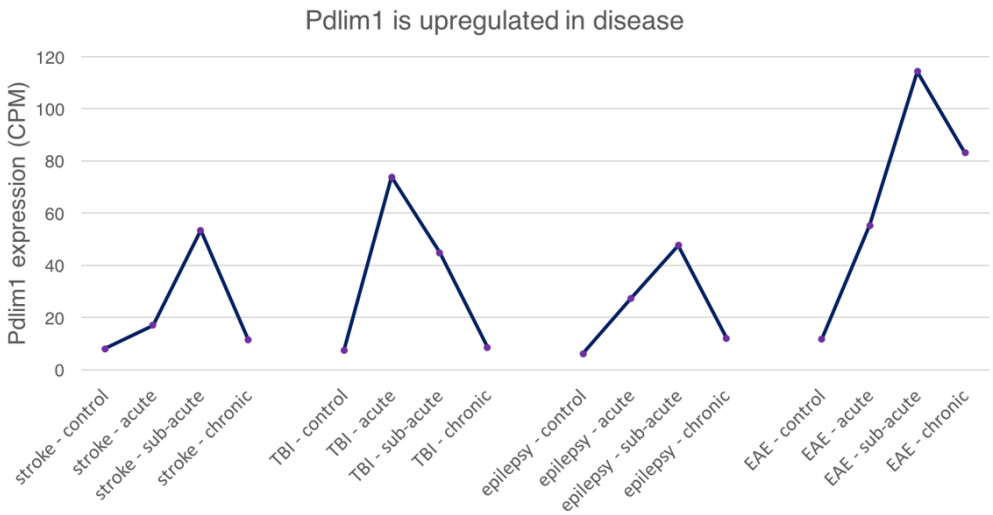

Figure 7: PDLIM1 is upregulated in disease
The graph is representing results of CNS endothelial cell purification followed by an RNA-Seq for PDLIM1 expression in different disease models. For each of the disease model, analysis was done at acute, subacute and chronic timepoint. Upregulation is the highest at subacute point in EAE, stroke and epilepsy and at acute timepoint in TBI. Y-axis is showing values in CPM = Counts Per Million.
EAE: Acute timepoint = first day that mice displayed a loss of 1 gram body weight; sub-acute timepoint= after the disability score levelled off for one day; chronic timepoint= two weeks after peak disease score. TBI: Timepoints - 24hours (acute), 72 hours (subacute) and 1 month (chronic) after cortical impact injury. Stroke: Timepoints - 24 hours (acute), 72 hours (subacute) and 1 month (chronic) after MCAO. Epilepsy: Timepoints - 3 hours (acute), 48 hours (subacute) and 1 month (chronic) post kainic acid injection. Kainic acid was used to induce seizures. Data is courtesy of Richard Daneman's laboratory at University of California, San Diego.

1.4 Project hypothesis and research questions

The project will research the role of a gene *Pdlim1* in regulating blood-brain barrier (BBB) dysfunction during neurological disease.

- Main hypothesis: Upregulation of PDLIM1 in brain endothelial cells leads to blood-brain barrier (BBB) dysfunction in neurological disease.
- Research questions:

• Where and when is PDLIM1 expressed?

We will use immunostaining methods to determine where and when is PDLIM1 expressed in health and during different disease models (EAE, epilepsy, TBI, stroke).

• Is PDLIM1 necessary for BBB dysfunction?

With a *Pdlim1* knockout mouse line, we will determine whether PDLIM1 is necessary for BBB dysfunction following induction of EAE, a model of multiple sclerosis.

• Is PDLIM1 sufficient for BBB dysfunction?

We will use a model of a doxycycline-regulated transgenic mouse model to overexpress PDLIM1 in CNS endothelial cells. Using this mouse model we will determine whether upregulation of PDLIM1 is sufficient to lead to BBB dysfunction.

• What is the molecular mechanism of PDLIM1?

This research question is very broad and in the project we will work only on establishing required cell lines needed for in vitro experiments. The focus will be on isolating and growing primary mouse brain endothelial cells (BECs) in culture. Expression of PDLIM1 in cell culture will be determined using immunostaining methods and Western blot. The goal is to optimize transfection process and conditions for a successful PDLIM1 siRNA knockdown in primary BECs.

2 Materials and methods

2.1 Animals (mice)

Mice were kept in Leichtag Biomedical Research Building (LBR) Basement at University of California, San Diego (UCSD). IACUC (Institutional Animal Care and Use Committee) oversees the UCSD animal care and use program. C57BL/6 mice were ordered from Jackson Laboratory or Charles River Laboratories. The *Pdlim1* knockout mice were purchased from Texas A&M Institute for Genomic Medicine (TIGM).

2.1.1 *Pdlim1* double transgenic mouse line

For *Pdlim1* double transgenic mice, Tet-Off expression system was employed. (Figure 8). Mouse line was made in the laboratory by my colleagues. *Pdlim1* gene was cloned into a construct containing the TRE (tetracycline response element) promoter, and IRES (internal ribosome entry site) sequence and the GFP reporter gene. Pronuclear injection was performed by the core facility at UCSD. Positive founders were mated to tTA mouse, and the offsprings that successfully transmitted and expressed the gene were used to start the line. *Pdlim1* transgenic mice were kept on doxycycline food pellets (5053 W/220 ppm Doxycycline, Cat# 1815011) to suppress *Pdlim1* gene expression. They were taken off doxycycline feeding as needed for experiments.

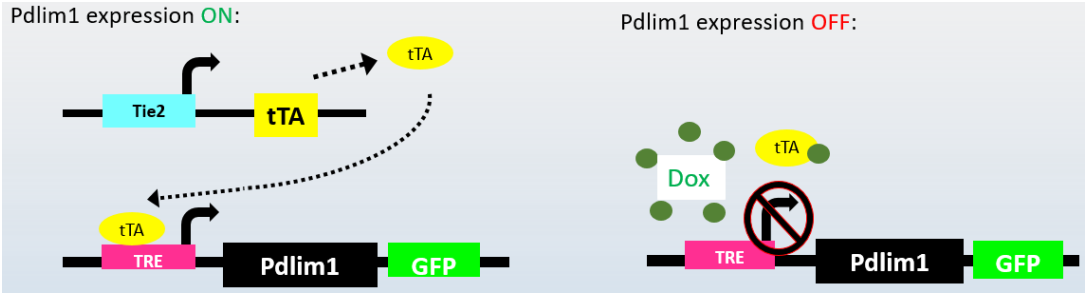

Figure 8: *Pdlim1* construct and control of gene expression
The *Pdlim1* gene is under the TRE (tetracycline- responsive promotor element) and the expression is regulated by tTA (tetracycline-controlled transactivator protein). tTA is under endothelial specific promoter Tie2. Binding of the tTA to TRE activates gene expression. Presence of doxycycline inhibits tTA binding and the expression is repressed.

2.2 Immunohistochemistry

2.2.1 Tissue isolation and preparation

For brain and spinal cord tissue isolation, mice were brought to the laboratory and anesthetized with 1,25 mL of Ketamine/xylazine mix (4mg/ml ketamine and 0,6mg/ml xylazine) injected intraperitoneally. Mice were given trans-cardiac perfusion with 1x DPBS for 2 min, followed by 4% paraformaldehyde for 5 min and 1x DPBS for 2 min. In case of trans-cardiac perfusion with biotin (0,4 mg/mL biotin in DPBS), it was done as following: 5 min biotin in DPBS, 6 min 4% paraformaldehyde, 1 min biotin in DPBS. Mice were dissected and brains and spinal cord were collected and cryopreserved in 30% sucrose at 4°C overnight. They were frozen in 2:1 30% sucrose:OCT and 10 micron sections were generated with Leica cryostat. Tissue sections were placed on micro slides (VWR, Superfrost® Plus, Cat. # 48311-703). Slides were kept at -80°C until the start of immunostaining.

2.2.2 Immunostaining of tissue slides

Slides were rehydrated for 2min in 1X PBS, followed by 5 min fixation in 4% paraformaldehyde. Slides were rinsed in 1X PBS and blocked/permeabilized with 10% normal goat serum in PBS + 0,2% triton-X for 40min on RT. After rinsing the slides in PBS, primary antibody (1:1000 dilution in antibody buffer - preparation in Annex 2) was added to the slides (100-200 μL per slide – to cover the tissue). They were incubated with primary antibodies overnight at 4°C. Slides were washed by transferring them between 1X PBS solutions (1x 1min, 2x 5min, 1x 10min). Secondary antibodies were diluted 1:1000 in 1X PBS. Slides were incubated with secondary antibodies (100-200 μL per slide – to cover the tissue) for 1,5h at RT. After washing the slides in 1X PBS (1x 1min, 2x 5min, 1x 10min), 2 drops of mounting medium DAPI fluoromount-G® were applied on them and cover slide was put on top. Sides of the cover slide were brushed with nail polish. Slides were left in the dark to dry and stored at 4°C.

2.2.3 Microscope imaging

For imaging of fluorescence labeled tissue, ZEISS Axio Imager.D2 in combination with computer program AxioVision was used.

2.3 Expression of PDLIM1 in health

To determine the expression pattern of PDLIM1 in brain and spinal cord in health, wild type C57BL/6 mice were given trans-cardiac perfusion with DPBS and PFA as described above. Brain and spinal cords were isolated and stained with antibodies against PDLIM1 and different cell types in blood-brain barrier. To check the specificity of PDLIM1 antibody, immunostaining against PDLIM1 was done on PDLIM1 knockout mouse tissue.

Table 1: BBB cell marker antibodies

Cell type	**Primary antibody**
Endothelial cells	CD31
Neurons	NeuN
Astrocytes	GFAP
Oligodendrocytes	CC1
OPC (oligodendrocytes precursor cells)	PDGFRa
Microglia	CD45
Pericytes	PDGFRb, CD13

2.4 BBB breakdown in disease

One part of practical work for this master thesis was done on tissue sections of mouse disease models of stroke, TBI, epilepsy and EAE. The experiments were performed by Daneman lab in 2015/2016 and sections were kept frozen at -80°C until the start of immunostaining.

2.4.1 PDLIM1 expression in stroke, TBI, epilepsy

All mice were given trans-cardiac perfusion with biotin. Immunostaining of slides was done according to the protocol using following antibodies:

Table 2: Used antibodies to determine PDLIM1 expression in disease models

Primary antibodies	Secondary antibodies
Rabbit α PDLIM1	Alexa Fluor® 594, Goat Anti-Rabbit IgG (H+L)
Rat α CD31	Alexa Fluor® 647, Goat Anti-Rat IgG (H+L)
	Streptavidin, Alexa Fluor® 488 (staining biotin)

2.4.1.1 Tracing in stroke, TBI and epilepsy

To determine the percentage of length of blood vessels with PDLIM1 in the area of leakage, slides were imaged and traced with computer program ImageJ.

For each disease model brain sections from 3 different mice were used. Images of leaky area and corresponding non leakage – control area on the same brain (or control brain in case of epilepsy) were taken on fluorescence microscope using 10x zoom. Tracing was done with computer program ImageJ. Exact area of leakage and corresponding non-leakage area was outlined for tracing (Figure 9).

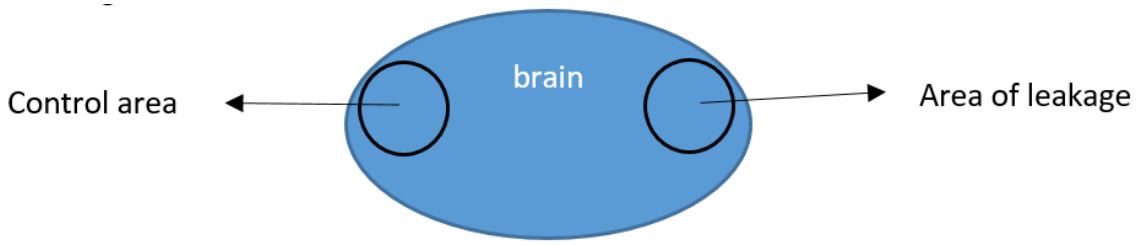

Figure 9: Scheme representation of areas used for tracing

In both areas each blood vessels was traced by measuring the length of it to get the total blood vessel length. For each traced blood vessel, it was determined if it is PDLIM1 + (by looking if there is a signal on second channel). Sum of length of blood

vessels with PDLIM1 divided by total blood vessel length was used for further analysis.

2.4.2 PDLIM1 expression in EAE

EAE induction in C57BL/6 mice was done in June, 2016 by my colleague Catie Profaci. All mice were given full dose of MOG and PTX and were trans-cardiac perfused with 488 labeled tomato lectin at different days after the disease onset– day 3, day 5 and day 7. Immunostaining of slides was done according to the protocol using following antibodies:

Table 3: Used antibodies to determine PDLIM1 expression in EAE

Primary antibodies	**Secondary antibodies**
Rb a PDLIM1	Alexa Fluor® 594, Goat Anti-Rabbit IgG (H+L)
Rat a CD31	Alexa Fluor® 647, Goat Anti-Rat IgG (H+L)

2.4.2.1 Tracing in EAE

To determine the percentage of length of blood vessels with PDLIM1; PDLIM1 and lectin; PDLIM1 and no lectin, slides were imaged and traced with computer program ImageJ.

Tracing was done on white matter of different spinal cord sections. At least two mice from each day were used for analysis.

First, each blood vessels was traced by measuring the length of it to get the total blood vessel length. For each traced blood vessel, it was determined if it is also PDLIM1 + (by looking if there is a signal on second channel), and the number of traced vessel was noted, if positive. In case if it was PDLIM1 + third channel was checked for lectin signal and the number of traced vessel was noted, if positive.

To get % of length of blood vessels with PDLIM1, sum of length of PDLIM1 + blood vessels was divided by total blood vessel length. $\frac{100x\ lenght\ PDLIM1+}{lenght\ CD31+}$

To get % of length of blood vessels with PDLIM1 and lectin, sum of length of PDLIM1 + and lectin + blood was divided by total blood vessel. $\frac{100x\ lenght\ PDLIM1+lectin+}{lenght\ CD31}$

To get % of length of blood vessels with PDLIM1 and no lectin, % of length of blood vessels with PDLIM1 and lectin was subtracted from % of vessels with PDLIM1.

$$\frac{100x\ lenght\ PDLIM1+}{lenght\ CD31+} - \frac{100x\ lenght\ PDLIM1+lectin+}{lenght\ CD31}$$

2.5 EAE in *Pdlim1* knockout mice

2.5.1 Induction of EAE

EAE (experimental autoimmune encephalomyelitis) was induced by active immunization using a Hooke Kit™ MOG_{33-55}/CFA Emulsion PTX (cat. no. EK- 2110). PTX (pertussis toxin) was prepared according to the protocol in the manufacturer instructions. Mice were anesthetized (inhaled anesthesia with isoflurane) prior of administration of MOG_{33-55} (myelin oligodendrocyte glycoprotein) in complete Freund's adjuvant (CFA) and PTX. Each mouse was administered 0,1mL of antigen emulsion (MOG) at upper and lower back subcutaneously (0,2 mL per mouse total), followed by an injection of PTX (0,1 mL i.p.) Second injection of PTX (0,1mL i.p.) was administered 24h later.

Induction of EAE with half dose was done using half amount of MOG (0,1 mL/mouse total) and PTX (0,05 mL i.p.). All the other steps were the same.

2.5.2 Clinical scoring in EAE mice

Mice were observed for 31 days after immunization. Everyday, each mouse was assigned a clinical score from 0 – 4 as described in the table 4. As soon as the first signs of paralysis occurred, food pellets and HydroGel (ClearH_20, Portland ME) were put on the floor of the cage.

Table 4: Score and corresponding clinical observation in EAE mice

Score	Clinical observation
0	No changes in motor function observed compared to non-immunized mouse
0,5	Tip of the tail is limp or Tail is fine, mouse is energetic, but small lag in flipping back is observed
1	Whole tail is limp
1,5	Limp tail and inability to extend back foot or Limp tail, mouse is energetic, but small lag in flipping back observed
2	Limp tail. When mouse is flipped on its back, it can't flip back or lag in flipping back is observed
2,5	Limp tail. Mouse is walking strange but still not dragging
3	Limp tail. Mouse is dragging. Hind legs still fine
3,5	Limp tail. Mouse is dragging. Paralysis of one hind leg or Limp tail. Mouse is dragging on the side, but can still move feet
4	Limp tail. Mouse is dragging. Paralysis of both hind legs

2.5.3 Quantification of CD4+ and CD8+ T cells

Mice were given trans-cardiac perfusion with DPBS and PFA at the end of experiment (day 31). Spinal cords were isolated and sectioned with cryostat. For each mouse, 5 different sections of spinal cord were used for counting. Slides were stained with antibodies against CD4 and CD8. Number of CD4+ and CD8+ cells was counted using manual cell counter. The average of all 5 sections per mouse was used for further analysis.

2.6 PDLIM1 overexpression *in vivo*

2.6.1 *Pdlim1* gene expression

To determine how long does it take for *Pdlim1* to start expressing in *Pdlim1* double transgenic mice (tTA-; TRE+), mice were taken off doxycycline feeding at 10 weeks of age and given trans-cardiac perfusion with DPBS and PFA at different days – day 7,8,9,10,13,14 after change of feed. For each day, one control mouse (tTA-; TRE-) was also perfused. Brain and spinal cords were isolated and stained against PDLIM1 and CD31 according to the protocol.

2.6.2 Analysis of overexpression

Female and male *Pdlim1* double transgenic (tTA+; TRE+) and control mice (tTA-; TRE-) were taken off doxycycline feed at 10 weeks of age. Mice were given trans-cardiac perfusion with biotin (methods section 2.3.1) at different timepoints – 11 days, 13, days, 15 days, 17 days, 38 days and 94 days after taking them off doxycycline feed. At least one male (+control) and one female mouse (+control) were analyzed at each timepoint as summarized in Table 5.

Table 5: Number and sex of mice used for each timepoint

Timepoint	Number of mice
11 days	1 male + 1 female
13 days	1 male + 1 female
15 days	2 males + 1 female
17 days	2 males + 3 females
38 days	2 males + 1 female
94 days	2 males + 1 female

Tissue slides with brains and spinal cord sections were stained against PDLIM1, CD31, Streptavidin, Iba1, CD45, CD13, GLUT-1 and GR-1 according to the protocol.

3 Results

3.1 Expression of PDLIM1 in health

To determine the expression of PDLIM1 in health, sections from C57BL/6 mice were immunostained against PDLIM1 and markers of different cell types - endothelial cells, neurons, astrocytes, oligodendrocytes, oligodendrocytes precursor cells, microglia and pericytes. To determine the specificity of PDLIM1 antibody, sections from *Pdlim1* knockout mice were stained against PDLIM1. We observed that in health there were very few blood vessels expressing PDLIM1 in brain or spinal cord (Figure 11). PDLIM1 expression was seen occasionally in a bigger blood vessel (not shown). Interestingly, there were many weakly PDLIM1 positive round cells in both brain and spinal cord, that co-localized with CC1, which is a marker for oligodendrocytes. PDLIM1/CC1 co-localization was detected in all areas of the brain, with the highest density observed in the areas of hypothalamus, thalamus, midbrain and pons (Figure 12, C1-C3). Furthermore, we also observed some neurons in the cerebral cortex of the brain showing weakly positive signal for PDLIM1 (not shown). Results of staining in spinal cord were similar, where both white and grey matter were positive for PDLIM1/CC1 signal, with more abundant PDLIM1/CC1 signal in the grey matter of spinal cord (Figure 13). Co-localization of PDLIM1 signal with any other cell type marker was not observed. PDLIM1 antibody specificity was confirmed because the staining of brain and spinal cord in knockout mouse showed no signal for PDLIM1 (Figure 10).

Taken together these results demonstrate the specificity of PDLIM1 antibody and that PDLIM1 is weakly expressed in CNS in health by oligodendrocytes. Weak signal is also observed in a small subset of neurons in the cerebral cortex and occasionally in bigger blood vessels in both brain and spinal cord.

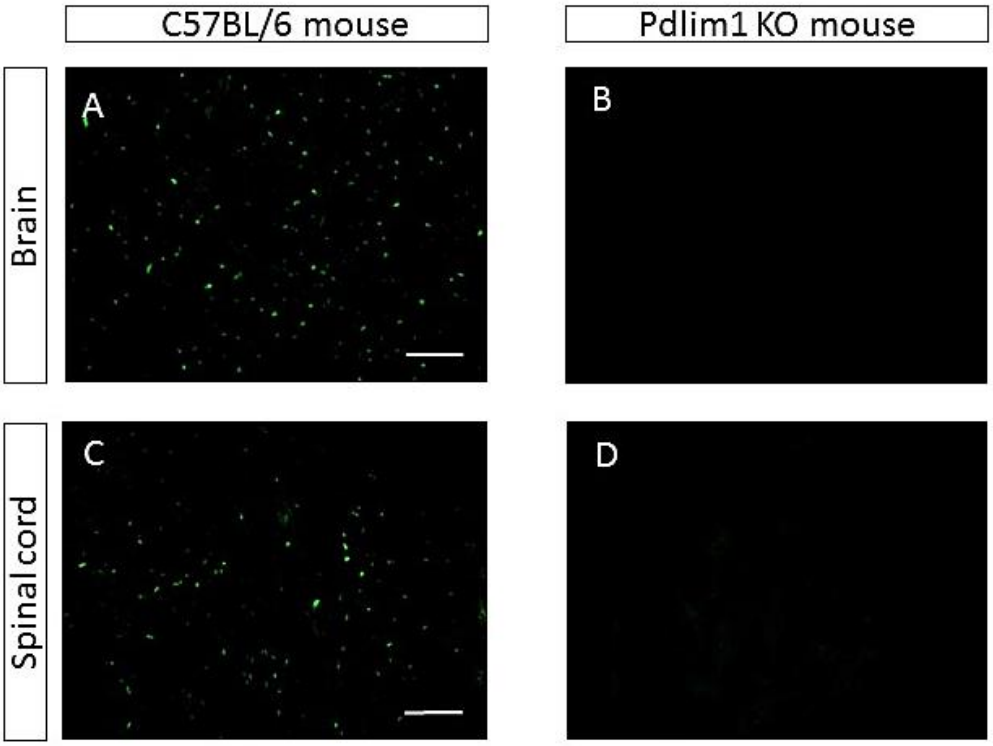

Figure 10: Specificity of PDLIM1 antibody.
Figure is showing immunostaining against PDLIM1 in pons region in the brain and grey matter of spinal cord in C57BL/6 and *Pdlim1* knockout mouse. PDLIM1 signal is seen in green in brain (A) and spinal cord section (C) of C57/BL/6 mouse and is absent in corresponding brain (B) and spinal cord (D) section of *Pdlim1* knockout mouse. Scale bar size is 100µm.

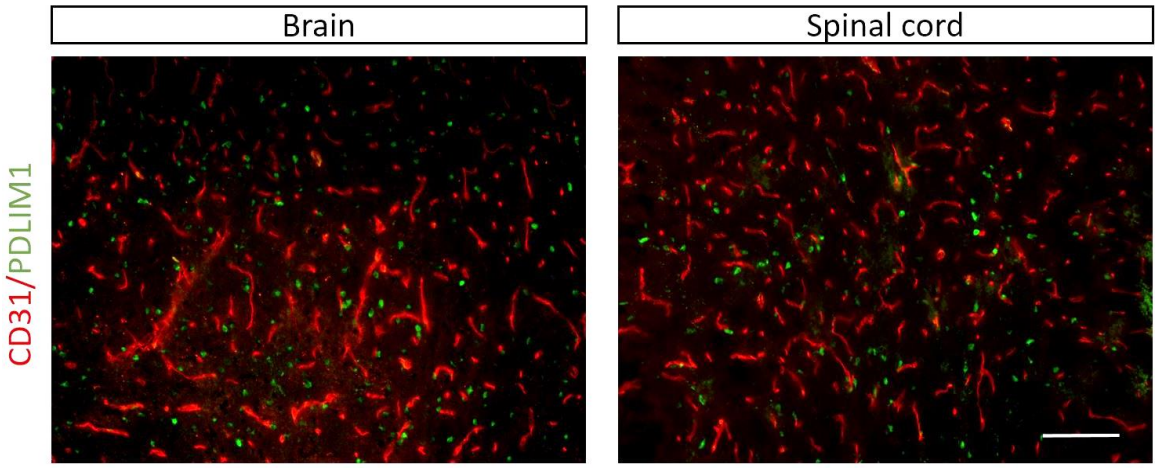

Figure 11: PDLIM1 is not expressed in blood vessels of the brain or spinal cord in health.
The figure is showing staining against PDLIM1 and CD31 in hypothalamus region of the brain and grey matter of spinal cord in health. CD31 is a marker for endothelial cells and is seen in red color. PDLIM1 signal is seen as small dots in green. No expression of PDLIM1 in blood vessels is observed. Scale bar size is 100µm.

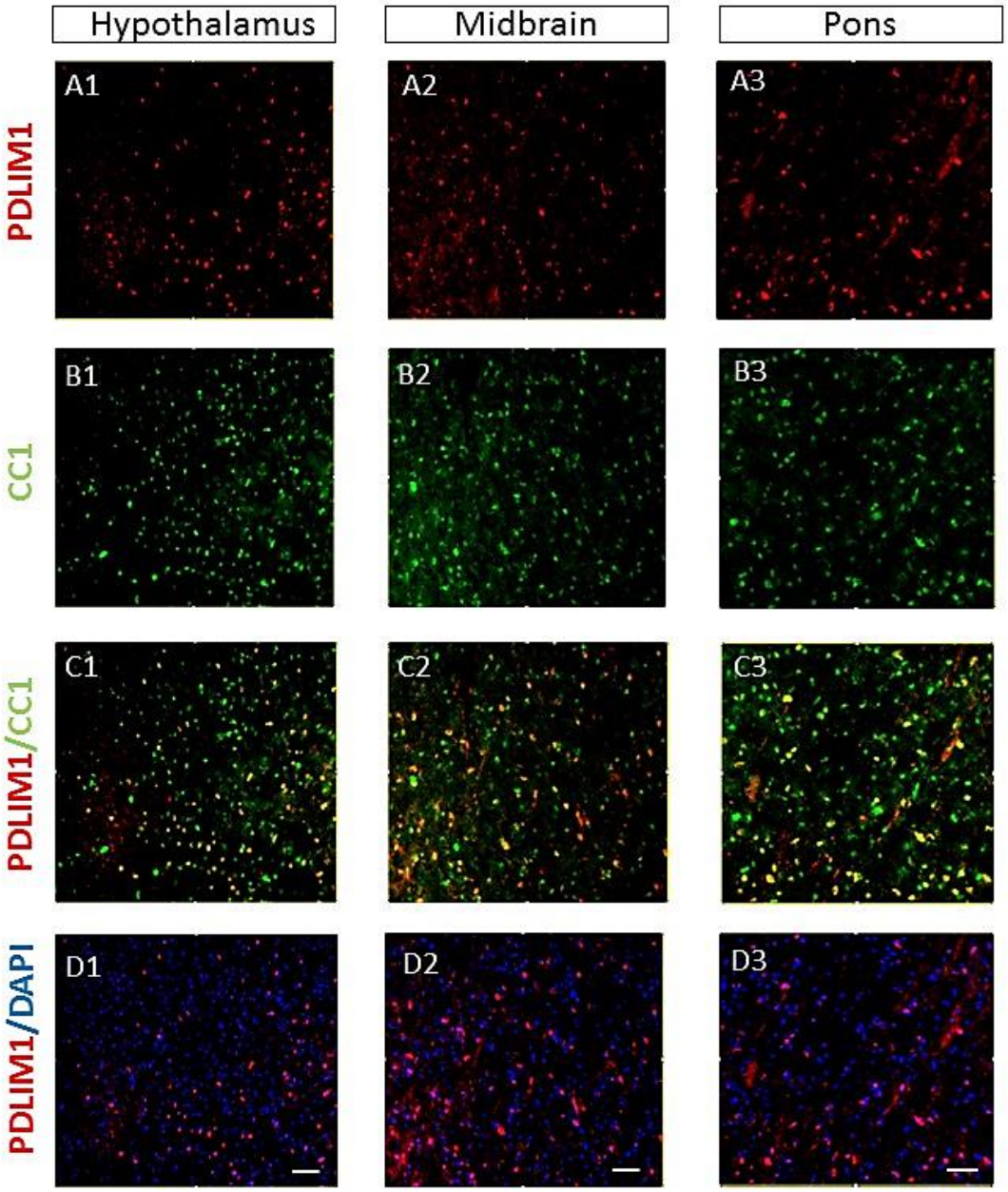

Figure 12: PDLIM1 is expressed by oligodendrocytes (CC1) in brain in health. Figure is showing results of immunostaining in three brain regions – hypothalamus, mid-brain and pons, where enriched PDLIM1 signal was observed compared to other brain regions. (A1-A3) Images are showing PDLIM1 signal in red color. (B1-B3) Images are showing CC1 signal in green color. (C1-C3) Co-localization between PDLIM1 (red) and CC1 (green) can be seen as yellow color. (D1-D4) Co-localization between PDLIM1 (red) and DAPI (blue) can be seen as pink color. DAPI is staining cell nucleus. Scale bar size is 50µm.

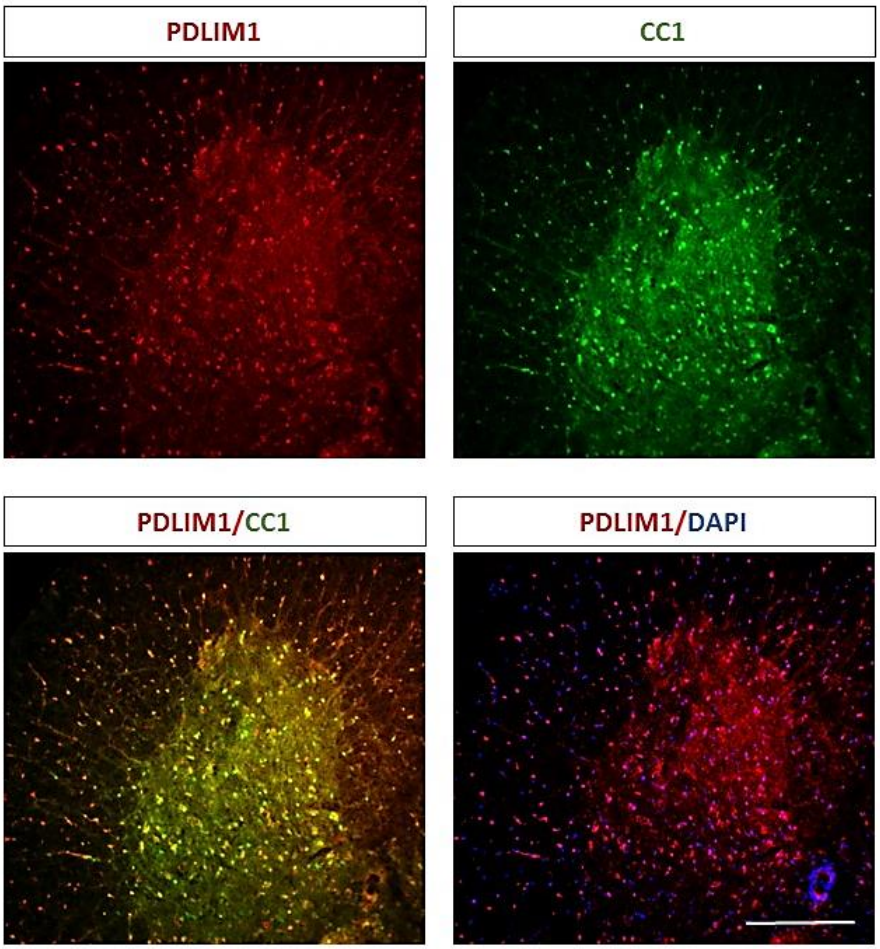

Figure 13: PDLIM1 is expressed by oligodendrocytes (CC1) in spinal cord in health.
Figure is showing results of immunostaining in one part of spinal cord. Grey matter of spinal cord is represented in the middle of each image and seen as more "dense" part. PDLIM1 (red) and CC1 (green) are shown as separate channels on the upper panel. Lower panel is representing merged channels, where co-localization between PDLIM1 and CC1 is seen as yellow color and between PDLIM1 and DAPI as pink color. DAPI is staining cell nucleus. Scale bar size is 200um.

3.2 Expression of PDLIM1 in stroke, TBI and epilepsy

On the basis of the finding that the gene *Pdlim1* is upregulated in BBB breakdown in the mouse models of stroke, TBI, and epilepsy (Figure 1), we investigated the expression pattern of PDLIM1 in each of above mentioned diseases. All mice were perfused with biotin at the end of the experiment. Biotin is a tracer molecule that we used to highlight the leakage as it leaks into the brain wherever there is an increased BBB permeability because of the BBB breakdown. Brain tissue sections were then stained with antibodies against PDLIM1, CD31 and biotin. BBB leakage was observed in each of the disease and is shown in the Figure 14 (1A-1C).

From the results of staining against PDLIM1 and CD31 (blood vessels) we observed that the expression of PDLIM1 was highly increased in the blood vessels only in the area of leakage in each of the disease models (Figure 14, A-C). Next, we quantified the percentage of blood vessels (endothelial cells) expressing PDLIM1 in the areas of leakage compared to the control areas for each of the diseases. For detailed description on quantification, refer to the methods section 2.5.1.1. The analysis showed that the percentage of blood vessels expressing PDLIM1 was the highest in stroke, with 98,8% in the area of leakage compared to the 2,4% in the control area (p= 1,50903E-08) (Figure 15). The results for epilepsy and TBI were almost the same, with 93,6% in the area of leakage compared to 7,4% in the control area for epilepsy (p= 4,20329E-07), and 93,5% in the area of leakage compared to the 8,8% in the control area for TBI (p= 1,75746E-06). All the results were statistically significant. Taken together these results confirmed the upregulation of *Pdlim1* in stroke, TBI, and epilepsy. PDLIM1 expression is highly increased in the blood vessels of the leakage area, with the highest percentage in stroke.

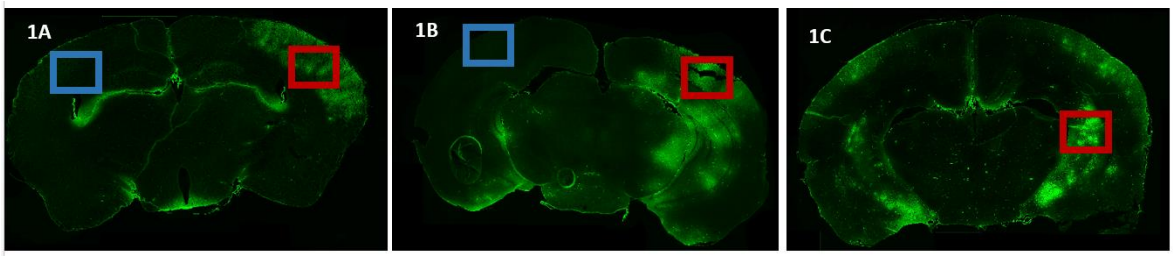

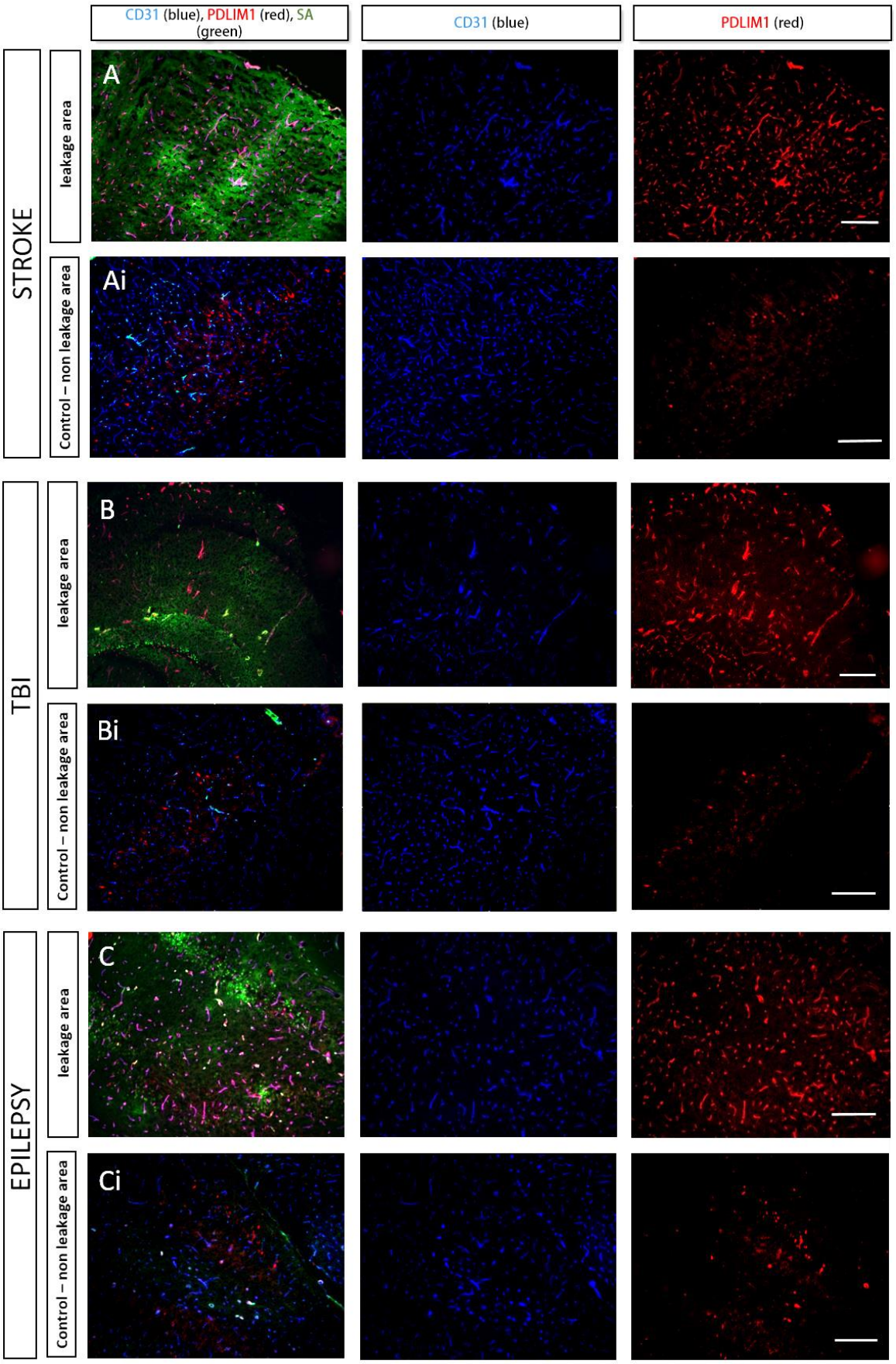
CD31 (blue), PDLIM1 (red), SA (green)
CD31 (blue)
PDLIM1 (red)
STROKE
leakage area
A
Control – non leakage area
Ai
TBI
leakage area
B
Control – non leakage area
Bi
EPILEPSY
leakage area
C
Control – non leakage area
Ci

Figure 14: PDLIM1 is upregulated in blood vessels in the area of leakage in stroke, TBI and epilepsy.
(1A, 1B, 1C) Images are showing mouse brains stained against biotin at subacute point in disease models of stroke (1A), TBI (1B) and epilepsy (1C). Green areas are representing BBB leakage. Red squares are outlining part of leakage areas and blue squares part of control non-leakage areas that are shown in higher zoom level on panels below.
(A,B,C) Zoomed in leakage areas are shown for stroke (A), TBI (B) and epilepsy (C). Biotin is stained in green, PDLIM1 in red and CD31 (blood vessels) in blue. Each panel is showing merged channels on the first image where co-localization of PDLIM1 and CD31 can be seen as pink color and separate channels for CD31 and PDLIM1.
(Ai, Bi, Ci) Corresponding zoomed in non-leakage control area are shown for stroke (Ai), TBI (Bi) and epilepsy (Ci). Scale bar size is 200µm.

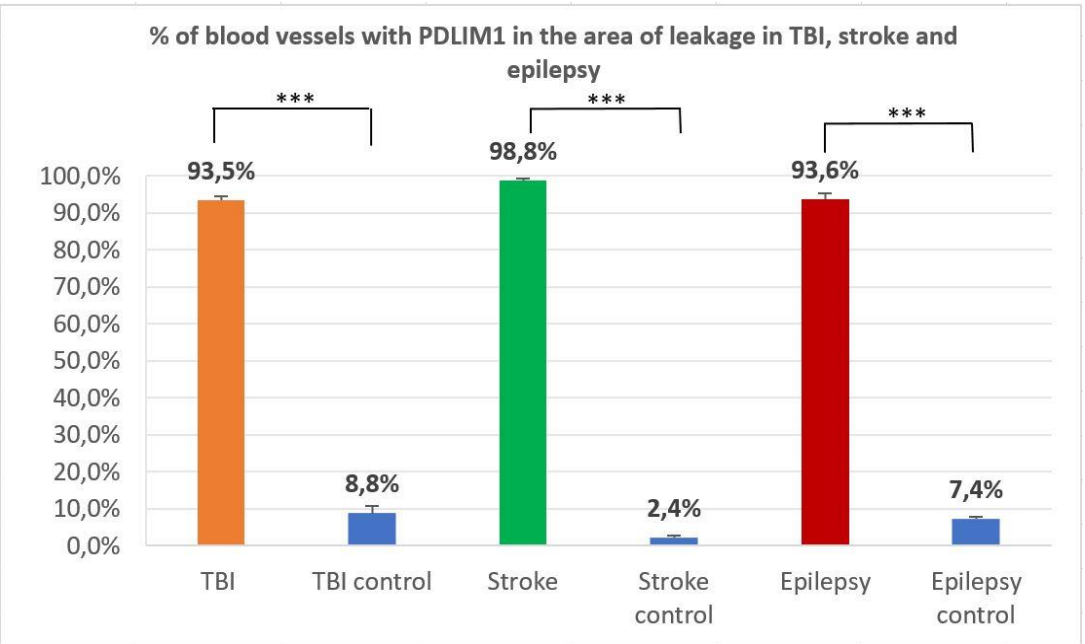

Figure 15: Percentage (%) of blood vessels with PDLIM1 in the area of leakage in stroke, TBI and epilepsy.
Results of tracing in disease models as described in method section (2.4.1.1) can be seen in orange for TBI, green for stroke and red for epilepsy. Blue bars are corresponding controls for each disease. Error bars are representing standard deviation. An unpaired (equal variance), one-tail t-test analysis was performed to assess the difference in each disease. ***Difference is statistically significant (P<0,001).

3.3 Expression of PDLIM1 in EAE

As the preliminary data showed that the upregulation of PDLIM1 was the highest in EAE compared to the other disease models, we investigated the expression pattern of PDLIM1 in EAE. Mice were perfused with fluorescently labeled tomato lectin at

day 3,5 and 7 after the onset of clinical symptoms. Perfusions with lectin were done to assess the perfusion efficiency. Whether the blood vessel was perfused or not signified if there are changes in the structural integrity of the vascular network. Following perfusion, spinal cord tissue sections were stained against PDLIM1, CD31 and DAPI (staining cell nucleus). We observed the increase in expression of PDLIM1 in the blood vessels in the white matter of spinal cord for all of the timepoints compared to the control (Figure 16). DAPI staining revealed areas with lesions, as the density of cells in a lesion is visibly higher due to immune cell infiltration. We observed that increase in expression of PDLIM1 was most abundant in the blood vessels in lesions (not shown).

Next, we quantified the percentage of blood vessels in the white matter that were PDLIM1 positive in control and day 3,5,7 after disease onset. For each of the PDLIM1 positive blood vessels we then determined whether it was perfused (positive for lectin). For a detailed description on how the tracing was done refer to the method section 2.5.2.1. Quantificational analysis presented in Figure 17 showed that in control 18% of blood vessels were PDLIM1 positive. 36,99% of those PDLIM1 positive vessels were unperfused. On day 3, 63,08% of blood vessels were PDLIM1 positive and 74,21% of those PDLIM1 positive vessels were unperfused. Highest percentage of blood vessels with PDLIM1 was at day 5 with 88,84% and 76,07% of PDLIM1 positive vessels were unperfused. On day 7, 67,91% of blood vessels were PDLIM1 positive with 63,14% of PDLIM1 positive vessels were unperfused. When compared to the control, statistically significant difference is only for day 5 ($p=0,04$) and day 7 (0,0000460). Difference between control and day 3 is not statistically significant ($p=0,13$), mostly due variation between mice as evident from the largest error bars for that day. Taken together, these results confirmed that PDLIM1 is upregulated in EAE. The upregulation is seen as increase in the blood vessels expressing PDLIM1 in the white matter of spinal cord, and is highest at day 5 after the onset of disease. With the increase in the % of blood vessels expressing PDLIM1, the perfusion efficiency in those blood vessels is decreasing.

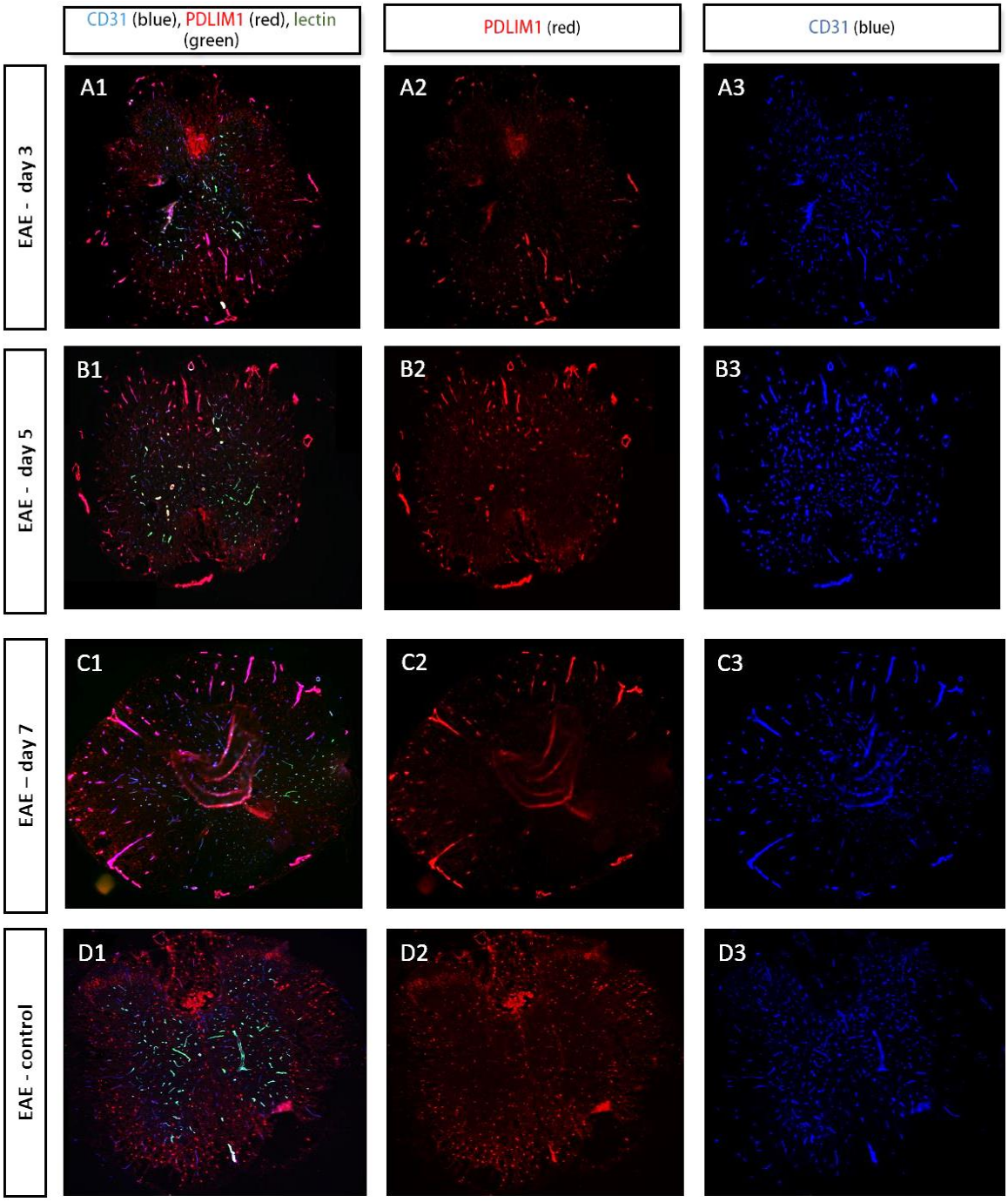

Figure 16: PDLIM1 expression in blood vessels is upregulated in EAE.
Figure is showing upregulation of PDLIM1 in spinal cord at day 3, 5, and 7 after the onset of disease. Mice where given trans-cardiac perfusion with fluorescently labeled tomato lectin (green), which binds to the endothelial cells inside the blood vessel. Each panel is representing different day after onset of disease. Control is shown on panel D. Merged channels for each day are seen on image 1 where co-localization between PDLIM1 (red) and CD31 (blue) can be seen as pink color. Separate channels are shown on image 2 (PDLIM1) and 3 (CD31). Images are courtesy of my colleague Catie Profaci**.**

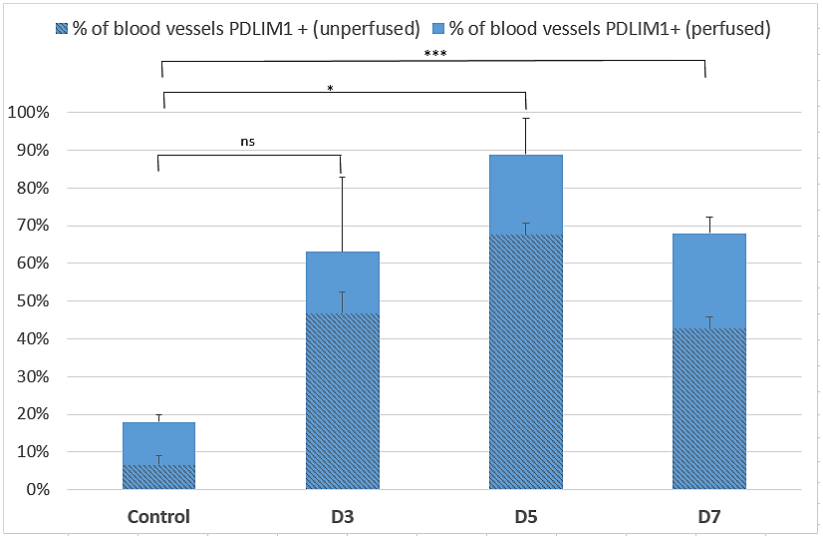

Figure 17: Percentage (%) of blood vessels with PDLIM1 in EAE – day 3,5, and 7. Graph is summarizing tracing results in EAE as described in method section (2.4.2.1). Percentage (%) of length blood vessels with PDLIM1 for each day is represented as whole bar. % of PDLIM1 positive blood vessels that were also positive for lectin, is shown as clear blue part of the bar. The presence of lectin is indicating perfusion of blood vessel. Shady part of the bar is representing % of length of blood vessels with PDLIM1 and no lectin (unperfused). Error bars are representing standard deviation. An unpaired (unequal variance), one-tail t-test analysis was performed to assess the difference between control and each day. Difference is statistically significant for *(P<0,05) and ***(P<0,001). NS = not significant

3.4 Induction of EAE

To investigate whether PDLIM1 is necessary for BBB dysfunction *in* vivo, EAE – a mouse model of multiple sclerosis was induced in the *Pdlim1* knockout mouse line. EAE was induced by active immunization with half or full dose of immunization agents MOG (myelin oligodendrocyte glycoprotein) and PTX (pertussis toxin). Half dose was given to make sure that that full dose was not masking the effect of *Pdlim1* genotype. Genotypes used for immunization with half dose were *Pdlim1* knockout (KO) mice, *Pdlim1* heterozygous (HET) mice *Pdlim1* wildtype (WT) mice. For immunization with full dose only KO and HET mice were used, because there were no WT litter mates available. Mice were observed for 31 days after the immunization and were assigned a clinical score from 0-4 every day. Spinal cord tissue sections were stained for CD4+ and CD8+ T cells to quantify inflammatory responses. For a detailed description of the immunization process, clinical scoring and counting analysis refer to methods section 2.5.

3.4.1 EAE immunization with half dose

The clinical scores of mice that received half dose of immunization agents are shown in Figure 18. We observed that all WT mice got sick (Figure 18B), while there were a few in the other groups that did not. Of those that did get sick in KO (Figure 18A) and HET (Figure 18C) group, some followed WT disease pattern while others showed more severe symptoms than WT. Analysis of average clinical scores by genotypes (Figure 19) revealed that KO mice had a similar pattern of disease onset compared to WT mice but showed lower clinical scores from day 18 on. HET mice had the latest onset of disease compared to WT and KO mice and the curve of clinical scores fell between the WT and KO mice afterwards. From the results of counting analysis of CD4+ and CD8+ cells we observed that the count for CD4+ cells was higher in all groups compared to the number of CD8+ cells, which was expected, as CD4+ cells are crucial for MS pathology (Figure 20). We also observed that the number of cells correlated with different average clinical scores of genotype groups on day 31. WT mice had the highest CD4+ and CD8+ counts compared to the other genotypes. As the WT mice also had the highest average clinical score on day 31, increased number of CD4+ and CD8+ cells was possibly correlated to higher inflammation in mice. Lowest cell count of CD4+ and CD8+ cells between groups was seen in KO mice. HET mice cell count fell between the WT and KO group.

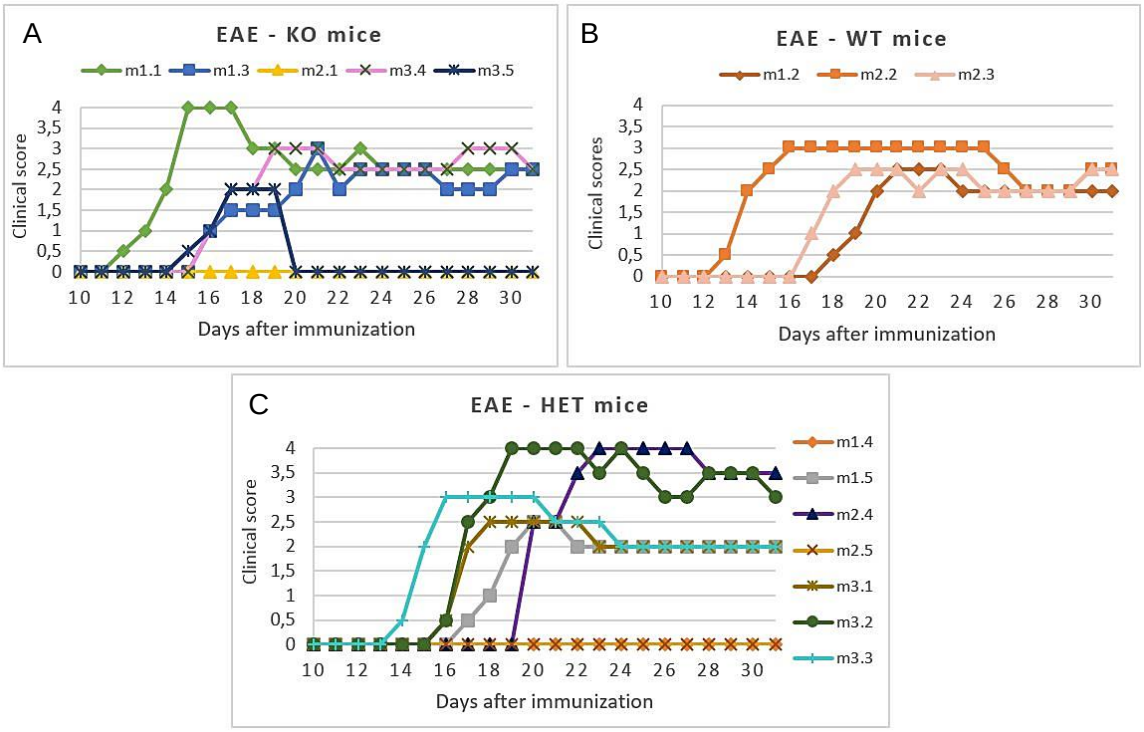

Figure 18: Clinical scores of *Pdlim1* KO, Het and WT mice in EAE.
Figure is showing clinical scores as a function of days after immunization with half dose in EAE for three mice genotypes – *Pdlim1* KO, Het and WT. Each genotype group is represented on a different graph. Only scores from day 10 on are shown, as there was no onset of disease before that. Each graph line is representing a different mouse and has a name that is used to differentiate between them (summarized in the legend).

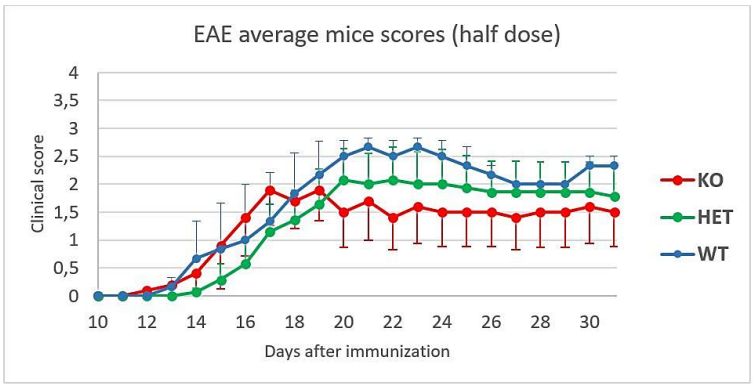

Figure 19: Average clinical scores of *Pdlim1* KO, Het and WT mice in EAE (half dose).
Average clinical scores for *Pdlim1* KO (n=5), Het (n=7) and WT (n=3) mice are shown as a function of days after immunization in EAE. KO mice group can be seen in red color, Het in green and WT in blue. Error bars are representing standard deviation.

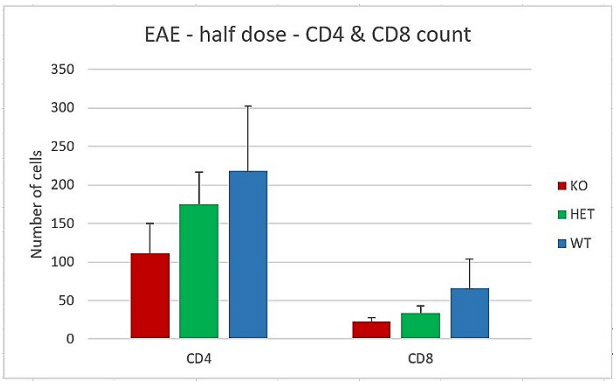

Figure 20: Number of CD4+ and CD8+ T cells in spinal cords of EAE mice (half dose).
The image is showing average number of CD4+ and CD8+ T cells at day 31 after immunization for *Pdlim1* KO (red), HET (green) and WT (blue) mice. Error bars are representing standard deviation.

3.4.2 EAE immunization with full dose

The clinical scores of *Pdlim1* KO and HET mice that received full dose of immunization agents are presented in Figure 21. All mice in both groups got sick or showed mild disease symptoms for a short period of time. We observed that there was a similar disease pattern for the majority of mice between both groups. The onset of disease for these mice was between day 12 – day 15 and they all reached peak of the disease between day 17 and day 21. Some of them showed signs of recovery after. Two mice in the KO group (Figure 21A) exhibited an interesting disease pattern. After the mice got sick, they got better or almost entirely better and then relapsed in the last days of the experiment. Similar disease pattern but with a shorter remittance was also observed in HET group (Figure 21B). Analysis of average clinical scores for the KO and HET group revealed almost the same clinical score curve until day 28. After that, KO group reached higher score when compared to the HET group (Figure 21C).

This obtained results showed some interesting disease patterns in both mice that received half and full dose of immunization agents. However, to make a conclusive judgement, we need to increase the n of each group

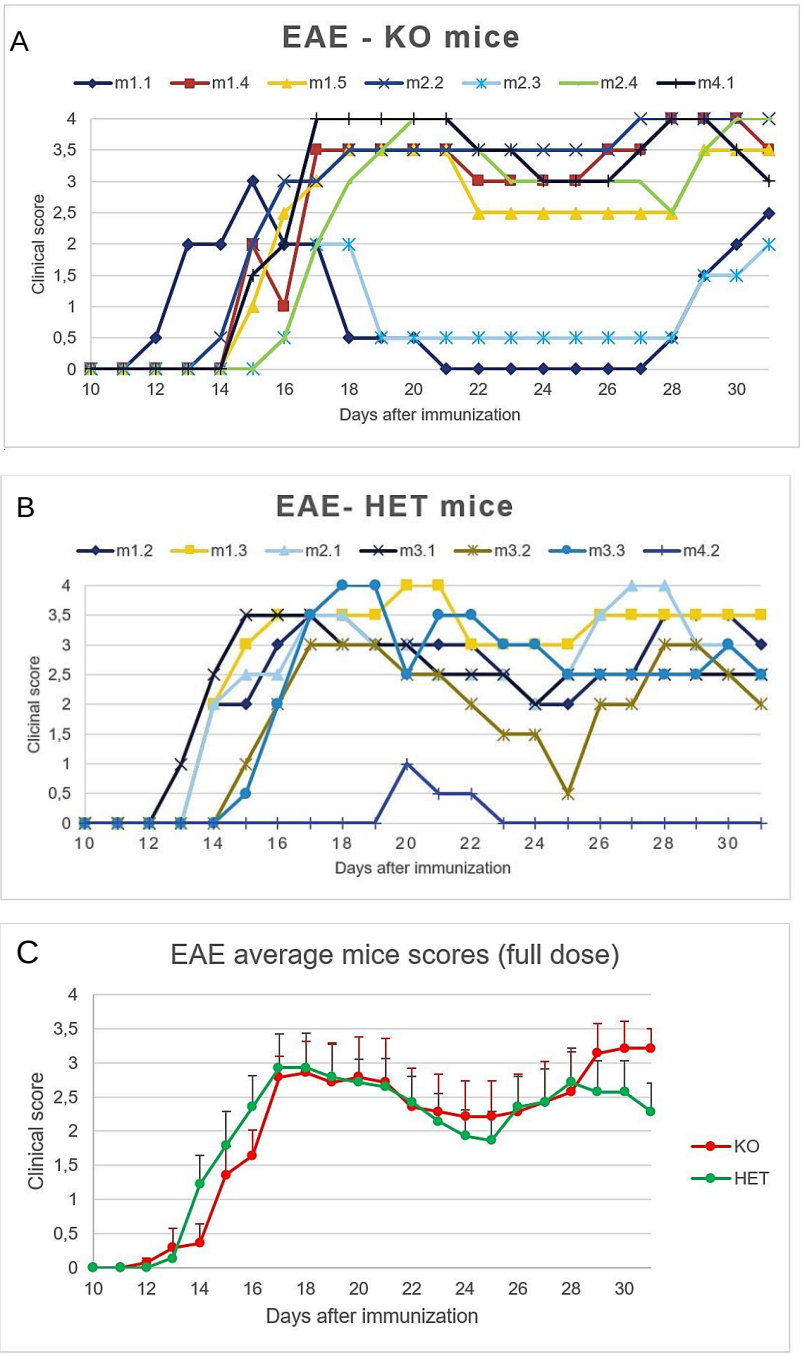

Figure 21: Clinical scores of *Pdlim1* KO and Het mice in EAE (full dose)
Figure is showing clinical scores as a function of days after immunization in EAE for two mice genotypes – *Pdlim1* KO (n=7), Het (n=7). Each genotype group is represented on a different graph. Only scores from day 10 on are shown, as there was no onset of disease before that. Each graph line is representing a different mouse and has a name that is used to differentiate between them (summarized in the legend). Average clinical scores for *Pdlim1* KO and Het mice are shown on the last image. KO mice group can be seen in red color and Het in green. Error bars are representing standard deviation.

.

3.5 PDLIM1 overexpression *in vivo*

To determine whether PDLIM1 is sufficient for BBB dysfunction *in vivo*, we generated a *Pdlim1* double transgenic mouse line overexpressing PDLIM1. For detailed description on how the line was generated and gene expression controlled, refer to methods sections 2.1.1 and 2.6. First, we investigated how many days was needed for PDLIM1 expression to turn on after taking the mice off doxycycline feed. Brains and spinal cords were collected at different timepoints and tissue sections were stained against PDLIM1 and CD31. To explore whether PDLIM1 overexpression had an effect at a specific time after the expression was on, we then chose different timepoints for immunohistochemistry analysis after the *Pdlim1* gene expression turned on, ranging from 1 day to 3 months (methods section 2.6). At each timepoint mice were perfused with biotin and brain and spinal cord tissue sections were stained against biotin, PDLIM1, CD31 (blood vessels), CD13 (pericytes), Iba1 (microglia), GLUT-1 (glucose transporter), GR-1 (neutrophils) and CD45 (macrophages).

We observed that blood vessels started expressing PDLIM1 at day 10 after taking mice off doxycycline feed (Figure 22). The expression was detected in all areas of the brain and spinal cord, but the number of blood vessels expressing PDLIM1 was higher in some areas (e.g. hypothalamus) compared to the others (e.g. midbrain). It should be mentioned that there was variation between mice in the days needed for expression to turn on and in expression pattern. In some mice, expression turned on around day 11 or day 12. The pattern of expression was also different in regard to the amount of blood vessels expressing PDLIM1 and areas of expression.

Next, we compared the number of blood vessels expressing PDLIM1 at different timepoints. We observed the lowest amount at days 11 and 13. From day 17 on, the increase was seen, peaking at day 38. Mice perfused at day 94 exhibited similar amounts to those at day 38 (not shown).

As PDLIM1 and GFP were under the same promoter, we investigated if there was co-localization between PDLIM1 and GFP expression in blood vessels (Figure 23).

We observed that majority of PDLIM1 positive blood vessels also expressed GFP. However, we also detected blood vessels expressing only PDLIM1 or only GFP, but the amount of them vas visibly lower.

Next we investigated whether PDLIM1 was causing leakage or if it had an effect on pericytes, microglia, neutrophils, macrophages or glucose transporter. From staining against pericytes and microglia no change was observed when compared to control (not shown). Pericytes were still covering the blood vessels expressing PDLIM1 at all timepoints (not shown). The microglia expression between double transgenic and control mice (not shorn) was also the same. Furthermore, no increase of neutrophils or macrophages was observed at any timepoint (not shown). Staining against biotin revealed no evidence of leakage at any timepoint. Blood vessels expressing PDLIM1 stayed intact and biotin was only detected in the lumen (not shown). Results from staining against GLUT-1 showed that blood vessels expressing PDLIM1 were also covered by glucose transporters (not shown).

Taken together this results demonstrate that our Tet-off expression system in *Pdlim1* double transgenic mice is working. The expression is not perfect as some of the blood vessels express only PDLIM1 or only GFP. PDLIM1 expression in blood vessels gradually increases from day 10 on after taking mice off doxycycline, with the highest expression at day 38 and 94. PDLIM1 overexpression does not cause leakage or has any effect on the cell types listed above at any timepoint that we investigated.

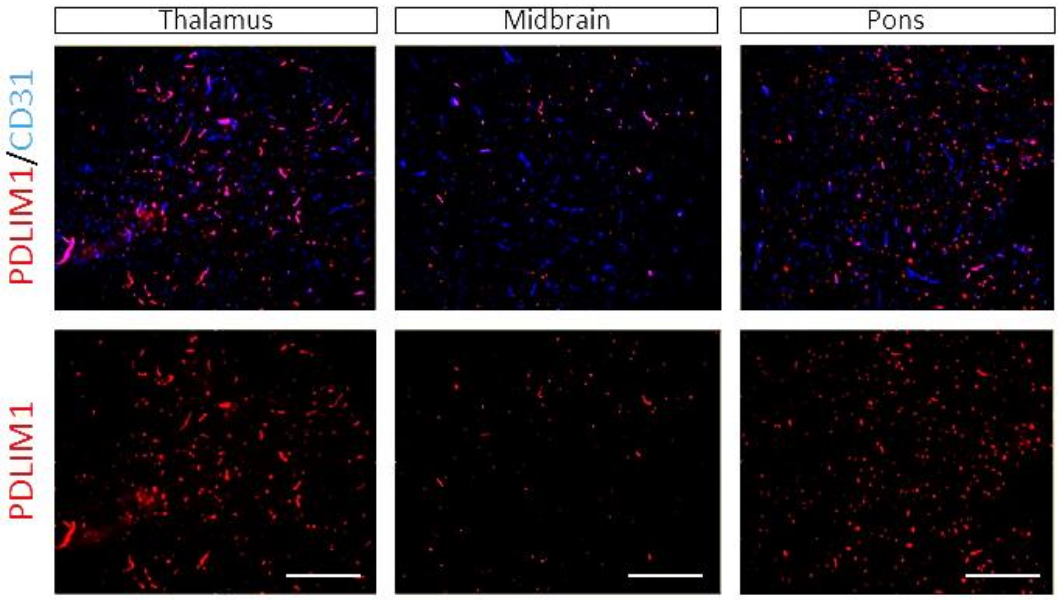

Figure 22: PDLIM1 expression starts at day 10 after taking mice off doxycycline feed. The figure is showing brain section of double transgenic mouse at day 10 after taking it off doxycycline feed. Images are representing three brain regions – thalamus, midbrain and pons stained against PDLIM1 and CD31. PDLIM1 is stained in red color and CD31 in blue. Co-localization of PDLIM1 and CD31 can be seen as pink color on the upper panel. Scale bar size is 200µm.

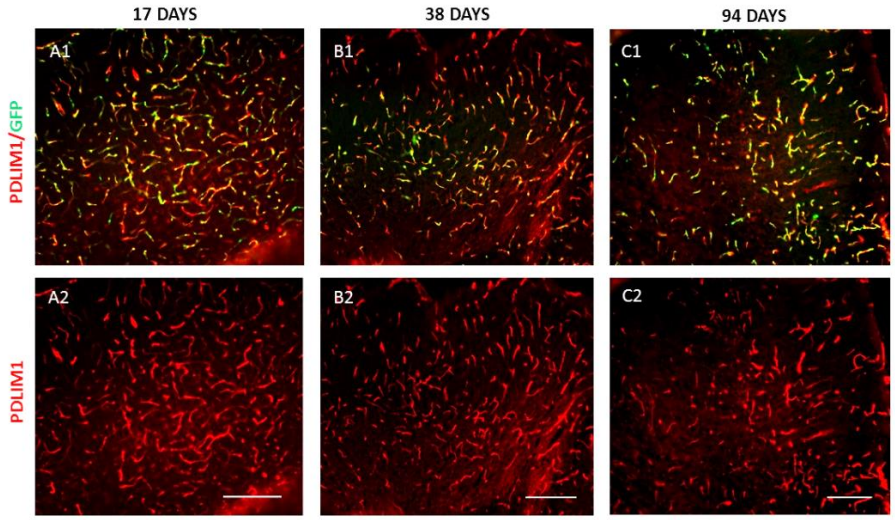

Figure 23: PDLIM1/GFP expression at different timepoints.
Figure is showing PDLIM1 and GFP expression in blood vessels at day 17, 38 and 94 after taking double transgenic mice off doxycycline. GFP and PDLIM1 are under the same promoter. The upper panel panel (A1, B1, C1) is showing merged images for each timepoint where PDLIM1 is stained in red, GPF in green and colocalization between them is seen as yellow color. Lower panel (A2, B2, C2) is showing only PDLIM1 signal of each merged picture. Scale bar size is 100 µm.

4 Discussion

The CNS vasculature expresses a series of unique properties known as the blood-brain barrier. This barrier tightly regulates the flow of ions, molecules and cells between the blood and the brain and is crucial for maintaining brain homeostasis thus allowing for proper neuronal function. BBB breakdown is a feature observed in many neurological diseases including multiple sclerosis, stroke, TBI and epilepsy. The molecular mechanisms of BBB breakdown are still not well understood and there are many questions yet to be answered. Better understanding of why and how BBB breakdown occurs is necessary for the treatment of neurological diseases as it would allow us to develop therapeutics aimed to limit the BBB breakdown or therapeutics able to cross the barrier. One particular question that we are interested in is whether there is a common pathway of the BBB breakdown and repair across all of the previously mentioned diseases. Our preliminary data identified a set of genes upregulated during BBB breakdown in all four diseases. One of these genes is *Pdlim1.* Previous studies identified PDLIM1 as a cytoskeletal protein that binds to actinin. Although the exact function of PDLIM1 remains unclear, recent work implicates its role in progression of breast cancer (Liu et al. 2015), glioma invasion (Ahn et al. 2016), induction of EMT (epithelial-mesenchymal transition) in colorectal cancer following PDLIM1 downregulation (Chen et al. 2016) and in NF-κ B-mediated inflammatory signaling, as a negative regulator (Ono et al. 2015). Here we suggest a novel role of PDLIM1 in BBB dysfunction in disease.

We started our study by first determining the expression pattern of PDLIM1 in health and disease models of stroke, EAE, TBI and epilepsy. Our PDLIM1 expression profile analysis in endothelial cells in health confirmed what was already known from the previous literature (te Velthuis & Bagowski 2007), that PDLIM1 is expressed at very low amounts in CNS compared to other tissue in the body. However, here we report for the first time that the low amount in CNS corresponds to expression of PDLIM1 by oligodendrocytes and occasionally large blood vessels.

One of the key findings in our study is a similar pattern of PDLIM1 expression in EAE, stroke, TBI and epilepsy. We showed PDLIM1 upregulation at acute and subacute timepoints in all of the diseases and also at the chronic timepoint in EAE. Upregulation in EAE, stroke and epilepsy is the highest at subacute point while in TBI the peak is at the acute timepoint. Common for all of these timepoints where PDLIM1 upregulation is the highest is that there is also significant vascular leakage (preliminary data). With further immunostaining analysis of subacute points of stroke, TBI and epilepsy we showed that Pdlim1 upregulation results in expression of PDLIM1 in the blood vessels in the areas of BBB breakdown. Moreover, tracing analysis revealed a significant difference in PDLIM1 expression in blood vessels between the leakage and control area in each of the disease. In fact, the expression is so high that in all of the diseases almost all of the blood vessels in the leakage area are expressing PDLIM1. Our analysis also revealed a similar expression pattern in spinal cords of EAE disease model. Here we investigated day 3, 5 and 7 after the onset of disease. PDLIM1 is seen in blood vessels in lesions at all days. Interestingly, we observed that the perfusion efficiency in PDLIM1 positive blood vessels is very low, indicating that these vessels have compromised vascular integrity and do not get perfused. However, low perfusion efficiency could also result from other influencing factors contributing to disease pathology and not PDLIM1. As PDLIM1 upregulation in EAE is still high at the chronic timepoint (2 weeks after peak disease score), further analysis is needed to determine the expression later in the disease. It would be interesting to look at perfusion efficiency at this timepoint, as this is something we haven't done. Together, our findings indicate a potential correlation between PDLIM1 and BBB dysfunction.

To elucidate the effect of PDLIM1 on the BBB we employed two *in vivo* models – *Pdlim1* knockout and *Pdlim1* double transgenic model. To answer our research question if PDLIM1 is necessary for BBB breakdown we induced an EAE disease model in *Pdlim1* KO mice. Even though no significant phenotype was found, our findings revealed rather interesting disease patterns in some KO and HET mice. Some of the mice did not get sick at all or showed mild disease symptoms for a short period of time, while some recovered almost completely before relapsing. One possible explanation is that here the absence of PDLIM1 is helping with mice recovery

by promoting myelination of damaged neurons. PDLIM1 was shown recently to inhibit beta-catenin mediated transcription by preventing its nuclear translocation (Chen et al. 2016). Moreover, Tawk et al. (2011) demonstrated that Wnt/B-catenin signaling is driving myelination in Schwann cells and oligodendrocytes. Perhaps the absence of PDLIM1 allows for more nuclear translocation of beta-catenin and higher transcription levels of myelin genes. As EAE is a demyelinating disease, this could lead to KO mice showing less severe disease symptoms or even signs of complete recovery.

In contrast, we observed some KO and HET mice with more severe disease clinical scores than WT mice. Given the existing knowledge about PDLIM1, we present two possible explanations. Ono et al. (2015) demonstrated that PDLIM1 prevents nuclear translocation of transcription factor p65, suggesting that it might have a role in suppressing NF-κ B-mediated signaling and inflammation. In this context, the absence of PDLIM1 could lead to higher inflammation in EAE mice. The second explanation stems from a recent study identifying an interaction between neurotrophin receptor $p75^{NTR}$ and PDLIM1. In the study they proposed PDLIM1 as a novel signaling adaptor for $p75^{NTR}$, and showed that PDLIM1/$p75^{NTR}$ interaction is needed for glioma invasion *in vitro* and *in vivo* (Ahn et al. 2016). Is it possible that PDLIM1/$p75^{NTR}$ interaction also plays a role in EAE disease progression? In another study, $p75^{NTR}$ expression was shown to turn on in endothelial cells following induction of EAE disease model and the $p75^{NTR}$ knockout mice exhibited more severe disease symptoms. Furthermore, in the knockout model, presence of T cells was higher while other immune cells were detected at lower amounts compared to the WT mice. Although the physiological role of this receptor in MS and EAE is not known, they suggested it might modulate BBB functions to restrict T cell invasion in EAE (Küst et al. 2006; Copray et al. 2004). This would explain why some of the Pdlim1 KO and HET mice in our experiments showed higher clinical scores compared to the WT. If PDLIM1 in fact acts as a signaling adaptor for $p75^{NTR}$ the absence of it may interfere with $p75^{NTR}$ signal transduction and leading to an outcome similar to that observed in $p75^{NTR}$ knockout mice.

However, although we observed some interesting disease patterns, they should be interpreted with caution as the variability of the data is very high. It is also difficult to

make a conclusive judgement from the data, first because of the low number of mice used in the experiment and second because some of them were immunized with half and some with full dose of immunization agents. For those immunized with full dose, there were no WT litter mates included in the experiment. However, the obtained average clinical scores from immunization with half dose showed very different disease pattern between genotype groups and we cannot rule out yet the possibility that higher dose of immunization agents might be masking the effect of PDLIM1. Future experiments should focus on obtaining more data to increase the n of all three genotypes from both immunization with half and full dose. In would be interesting to see if any of the disease patterns repeat in a large number of mice, indicating a possible phenotype. We conclude here that PDLIM1 is not necessary for BBB breakdown but it might have a role in severity of EAE disease progression.

To investigate the second research question of whether PDLIM1 is sufficient for BBB dysfunction *in vivo,* we employed a *Pdlim1* double transgenic mice model that overexpresses PDLIM1 in endothelial cells and analyzed several timepoints ranging from 1 day to 3 months after the initiation of PDLIM1 expression. However we did not observe BBB dysfunction at any point, thus we conclude that PDLIM1 is not sufficient for BBB dysfunction. Furthermore there was also no difference with control observed in number or morphology of microglia, pericytes, neutrophils, macrophages and GLUT-1. It is very likely that PDLIM1 overexpression in health has no effect on the BBB or other cells present. It is also possible that we did not analyze the right timepoints and elements that PDLIM1 might be influencing or that there is not enough PDLIM1 overexpressed to cause an effect. Future work will look into gene expression changes by performing a RNA-Seq analysis on endothelial cells following PDLIM1 overexpression.

Although not described in this research report one part of the project focused on establishing cell lines to explore the mechanism of PDLIM1 *in vitro*. We were successful in optimizing parameters for PDLIM1 siRNA knockdown in primary brain endothelial cells (BECs), however further work is needed to establish transfected primary BECs overexpressing PDLIM1. *In vitro* experiments will then test the involvement of PDLIM1 in two signaling pathways of interest - Wnt/beta-catenin signaling and NF-κ B-mediated signaling, by treating the cell lines with Wnt and TNF-alpha

and subsequently checking for changes in cell proliferation, expression of BBB markers (tight junctions, vesicles, expression of transporters and leukocyte adhesion molecules) or downstream markers of both pathways. We hope that *in vitro* experiments will help us understand what might be the function of PDLIM1 at the BBB *in vivo*.

In summary, we demonstrated that there is a possible correlation between PDLIM1 and BBB dysfunction. We analyzed the expression of PDLIM1 in CNS in health and four disease models – EAE, stroke, TBI and epilepsy at the time of BBB breakdown. We found that expression is highly upregulated in the blood vessels in the area of BBB breakdown in all disease models, but remained at low levels in health, with a negligible number of PDLIM1 positive blood vessels. From the findings of our *in vivo* studies it seems that PDLIM1 is not necessary or sufficient for BBB breakdown. Taken together, these results would seem to suggest that upregulation of PDLIM1 does not lead to BBB dysfunction. However, even though we did not observe any effect when overexpressing PDLIM1 *in vivo*, data from inducing the EAE disease model in *Pdlim1* knockout mice is more promising. Future work needs to be carried out to address the possibility that PDLIM1 plays a role in inflammation upon BBB breakdown or is involved in myelination process in EAE. However, some questions still remain unanswered. What is the role of PDLIM1 at the BBB in all of these diseases? If PDLIM1 does not contribute to BBB dysfunction, is it possible that it protects BBB integrity or is involved in BBB repair? As *Pdlim1* was previously identified in a set of genes upregulated during BBB breakdown, understanding its function could help us answer the bigger questions about the underlying mechanisms of BBB breakdown and repair in disease. Ultimately this would open new possibilities for treatment options of neurological diseases where BBB breakdown is a major contributing factor.

List of References

Abbott, N.J. et al., 2010. Structure and function of the blood–brain barrier. *Neurobiology of Disease*, 37(1), pp.13–25.

Ahn, B.Y. et al., 2016. Glioma invasion mediated by the p75 neurotrophin receptor (p75NTR/CD271) requires regulated interaction with PDLIM1. *Oncogene*, 35(11), pp.1411–1422.

Alluri, H. et al., 2015. Blood–brain barrier dysfunction following traumatic brain injury. *Metabolic Brain Disease*, 30(5), pp.1093–1104.

Alvarez, J.I., Cayrol, R. & Prat, A., 2011. Disruption of central nervous system barriers in multiple sclerosis. *Biochimica et Biophysica Acta (BBA) - Molecular Basis of Disease*, 1812(2), pp.252–264.

Attwell, D. et al., 2010. Glial and neuronal control of brain blood flow. *Nature*, 468(7321), pp.232–43.

Bauer, K. et al., 2000. Human CLP36, a PDZ-domain and LIM-domain protein, binds to alpha-actinin-1 and associates with actin filaments and stress fibers in activated platelets and endothelial cells. *Blood*, 96(13), pp.4236–45.

Bradl, M. & Lassmann, H., 2009. Progressive multiple sclerosis. *Seminars in Immunopathology*, 31(4), pp.455–465.

Brightman, M.W. & Reese, T.S., 1969. Junctions Between Intimately Apposed Cell Membranes in the Vertebrate Brain.

Chen, H.N. et al., 2016. PDLIM1 stabilizes the E-Cadherin/b-catenin complex to prevent epithelial-mesenchymal transition and metastatic potential of colorectal cancer cells. *Cancer Research*, 76(5), pp.1122–1134.

Copray, S. et al., 2004. Deficient p75 low-affinity neurotrophin receptor expression exacerbates experimental allergic encephalomyelitis in C57/BL6 mice. *Journal of Neuroimmunology*, 148(1–2), pp.41–53.

Daneman, R. et al., 2010. Pericytes are required for blood–brain barrier integrity during embryogenesis. *Nature*, 468(7323), pp.562–566.

Daneman, R., 2012. The blood-brain barrier in health and disease. *Annals of Neurology*, 72(5), pp.648–672.

Daneman, R. et al., 2009. Wnt/beta-catenin signaling is required for CNS, but not non-CNS, angiogenesis. *Proceedings of the National Academy of Sciences of the United States of America*, 106(2), pp.641–6.

Daneman, R. & Prat, A., 2015. The blood-brain barrier. *Cold Spring Harbor perspectives in biology*, 7(1), p.a020412.

Donkin, J.J. et al., 2009. Substance P is Associated with the Development of Brain Edema and Functional Deficits after Traumatic Brain Injury. *Journal of Cerebral*

Blood Flow & Metabolism, 29(8), pp.1388–1398.

Ehrlich, P., 1885. *Das Sauerstoff-Bedürfniss des Organismus : eine farbenanalytische Studie*, Berlin: August Hirschwald.

Erickson, M.A. & Banks, W.A., 2013. Blood–Brain Barrier Dysfunction as a Cause and Consequence of Alzheimer's Disease. *Journal of Cerebral Blood Flow & Metabolism*, 33(10), pp.1500–1513.

Evans, M.C. et al., 2013. Inflammation and neurovascular changes in amyotrophic lateral sclerosis. *Molecular and Cellular Neuroscience*, 53, pp.34–41.

Frohman, E.M., Racke, M.K. & Raine, C.S., 2006. Multiple Sclerosis — The Plaque and Its Pathogenesis. *New England Journal of Medicine*, 354(9), pp.942–955.

Garbuzova-Davis, S. et al., 2012. Impaired blood–brain/spinal cord barrier in ALS patients. *Brain Research*, 1469, pp.114–128.

Gloor, S.M. et al., 2001. Molecular and cellular permeability control at the blood–brain barrier. *Brain Research Reviews*, 36(2), pp.258–264.

Guttmann, C.R. et al., 2016. Multiple sclerosis lesion formation and early evolution revisited: A weekly high-resolution magnetic resonance imaging study. *Multiple Sclerosis Journal*, 22(6), pp.761–769.

Haj-Yasein, N.N. et al., 2011. Glial-conditional deletion of aquaporin-4 (Aqp4) reduces blood-brain water uptake and confers barrier function on perivascular astrocyte endfeet. *Proceedings of the National Academy of Sciences of the United States of America*, 108(43), pp.17815–20.

Harris, J.O. et al., 1991. Serial gadolinium-enhanced magnetic resonance imaging scans in patients with early, relapsing-remitting multiple sclerosis: Implications for clinical trials and natural history. *Annals of Neurology*, 29(5), pp.548–555.

Hasegawa, T. et al., 2010. CLP36 interacts with palladin in dorsal root ganglion neurons. *Neuroscience Letters*, 476(2), pp.53–57.

Hawkins, B.T. & Davis, T.P., 2005. The Blood-Brain Barrier/Neurovascular Unit in Health and Disease. *Pharmacological Reviews*, 57(2).

Heye, A.K. et al., 2014. Assessment of blood–brain barrier disruption using dynamic contrast-enhanced MRI. A systematic review. *NeuroImage: Clinical*, 6, pp.262–274.

Huang, Z.G. et al., 1999. Biphasic opening of the blood-brain barrier following transient focal ischemia: effects of hypothermia. *The Canadian journal of neurological sciences. Le journal canadien des sciences neurologiques*, 26(4), pp.298–304.

Kirk, J. et al., 2003. Tight junctional abnormality in multiple sclerosis white matter affects all calibres of vessel and is associated with blood-brain barrier leakage and active demyelination. *The Journal of Pathology*, 201(2), pp.319–327.

Kotaka, M. et al., 2000. Interaction of hCLIM1, an enigma family protein, with ?-

actinin 2. *Journal of Cellular Biochemistry*, 78(4), pp.558–565.

Kuroiwa, T. et al., 1985. The biphasic opening of the blood-brain barrier to proteins following temporary middle cerebral artery occlusion. *Acta Neuropathologica*, 68(2), pp.122–129.

Küst, B. et al., 2006. Deficient p75 low-affinity neurotrophin receptor expression does alter the composition of cellular infiltrate in experimental autoimmune encephalomyelitis in C57BL/6 mice. *Journal of Neuroimmunology*, 174(1–2), pp.92–100.

Liu, Z. et al., 2015. PDZ and LIM domain protein 1(PDLIM1)/CLP36 promotes breast cancer cell migration, invasion and metastasis through interaction with α-actinin. *Oncogene*, 34(10), pp.1300–1311.

Löscher, W. & Potschka, H., 2005. Blood-brain barrier active efflux transporters: ATP-binding cassette gene family. *NeuroRx : the journal of the American Society for Experimental NeuroTherapeutics*, 2(1), pp.86–98.

Lou, N. et al., 2016. Purinergic receptor P2RY12-dependent microglial closure of the injured blood-brain barrier. *Proceedings of the National Academy of Sciences of the United States of America*, 113(4), pp.1074–9.

Luissint, A.-C. et al., 2012. Tight junctions at the blood brain barrier: physiological architecture and disease-associated dysregulation. *Fluids and barriers of the CNS*, 9(1), p.23.

Marchi, N. et al., 2007. Seizure-Promoting Effect of Blood?Brain Barrier Disruption. *Epilepsia*, 48(4), pp.732–742.

McCarthy, D.P., Richards, M.H. & Miller, S.D., 2012. Mouse models of multiple sclerosis: experimental autoimmune encephalomyelitis and Theiler's virus-induced demyelinating disease. *Methods in molecular biology (Clifton, N.J.)*, 900, pp.381–401.

Minagar, A. & Alexander, J.S., 2003. Blood-brain barrier disruption in multiple sclerosis. *Multiple sclerosis (Houndmills, Basingstoke, England)*, 9(6), pp.540–9.

Nag, S., Manias, J.L. & Stewart, D.J., 2009. Pathology and new players in the pathogenesis of brain edema. *Acta Neuropathologica*, 118(2), pp.197–217.

Oby, E. & Janigro, D., 2006b. The Blood-Brain Barrier and Epilepsy. *Epilepsia*, 47(11), pp.1761–1774.

Ohno, K. et al., 2009. Characterization of CLP36/Elfin/PDLIM1 in the nervous system. *Journal of Neurochemistry*, 111(3), pp.790–800.

Ono, R., Kaisho, T. & Tanaka, T., 2015. PDLIM1 inhibits NF-κB-mediated inflammatory signaling by sequestering the p65 subunit of NF-κB in the cytoplasm. *Scientific Reports*, 5, p.18327.

Padden, M. et al., 2007. Differences in expression of junctional adhesion molecule-A and β-catenin in multiple sclerosis brain tissue: increasing evidence for the

role of tight junction pathology. *Acta Neuropathologica*, 113(2), pp.177–186.

Rubin, L.L. & Staddon, J.M., 1999. THE CELL BIOLOGY OF THE BLOOD-BRAIN BARRIER. *Annual Review of Neuroscience*, 22(1), pp.11–28.

Sandoval, K.E. & Witt, K.A., 2008. Blood-brain barrier tight junction permeability and ischemic stroke. *Neurobiology of Disease*, 32(2), pp.200–219.

Saunders, N.R. et al., 2014. The rights and wrongs of blood-brain barrier permeability studies: a walk through 100 years of history. *Frontiers in neuroscience*, 8, p.404.

Sorokin, L., 2010. The impact of the extracellular matrix on inflammation. *Nature Reviews Immunology*, 10(10), pp.712–723.

Tawk, M. et al., 2011. Wnt/beta-catenin signaling is an essential and direct driver of myelin gene expression and myelinogenesis. *The Journal of neuroscience : the official journal of the Society for Neuroscience*, 31(10), pp.3729–42.

Unterberg, A.W. et al., 2004. Edema and brain trauma. *Neuroscience*, 129(4), pp.1019–1027.

Vallenius, T. et al., 2004. The PDZ-LIM protein RIL modulates actin stress fiber turnover and enhances the association of α-actinin with F-actin. *Experimental Cell Research*, 293(1), pp.117–128.

Vallenius, T., Luukko, K. & Mäkelä, T.P., 2000. CLP-36 PDZ-LIM protein associates with nonmuscle alpha-actinin-1 and alpha-actinin-4. *The Journal of biological chemistry*, 275(15), pp.11100–5.

te Velthuis, A.J.W. & Bagowski, C.P., 2007. PDZ and LIM domain-encoding genes: molecular interactions and their role in development. *TheScientificWorldJournal*, 7, pp.1470–92.

De Vivo, D.C. et al., 1991. Defective Glucose Transport across the Blood-Brain Barrier as a Cause of Persistent Hypoglycorrhachia, Seizures, and Developmental Delay. *New England Journal of Medicine*, 325(10), pp.703–709.

Wang, H. et al., 1995. *Cloning of a rat cDNA encoding a novel LIM domain protein with high homology to rat RIL*,

Winkler, E. a, Bell, R.D. & Zlokovic, B. V, 2011. Central nervous system pericytes in health and disease. *Nature neuroscience*, 14(11), pp.1398–1405.

Zhao, Z. et al., 2015. Establishment and Dysfunction of the Blood-Brain Barrier. *Cell*, 163(5), pp.1064–1078.

Zlokovic, B. V., 2008. The Blood-Brain Barrier in Health and Chronic Neurodegenerative Disorders. *Neuron*, 57(2), pp.178–201.

del Zoppo, G.J. et al., 2006. Vascular matrix adhesion and the blood-brain barrier. *Biochemical Society Transactions*, 34(6), pp.1261–1266.